

Master Thesis- Master Sustainable Development

P³: Promoting Peatland Potential

What are the effects of restoration measures on plant types in a degraded raised bog: The Fochteloërveen case study.



Restored bog at the Fochteloërveen, O'Donovan. J 2024

Name: Julianne O'Donovan

Student number: 2720906

Supervisor: Dr. Ralph J.M. Temmink

Second reader: Dr. Jerry van Dijk

Date: 4th October, 2024

Abstract

Anthropogenic impacts, including rising temperatures from fossil fuel emissions, widespread air and water pollution, and land use changes for farming and urbanization, have led to extensive destruction and degradation of critical landscapes. Bogs, in particular, are at risk, as they provide essential ecosystem services such as water purification, flood control, carbon storage, and recreation. The loss of these areas can be disastrous, releasing significant volumes of terrestrial carbon and undermining climate action efforts. In the Netherlands, restoration initiatives have been ongoing to try recover some of the once-extensive peatlands in the northern regions, where now only small fragments remain. Effective monitoring of these restoration techniques is vital for evaluating their success and informing future applications.

This study investigates the impact of innovative restoration methods, specifically peat inversion, on *Sphagnum* recovery and *Molinea* reduction in the Fochteloërveen bog remnant. Utilizing drone surveying combined with Random Forest classification, two sites that underwent peat inversion in 2000 and 2023 were compared with a control site. The classification accuracy reached 88%, effectively distinguishing fine-scale vegetation features. Results indicated that the 2000 inverted site did not have more *Sphagnum* or less *Molinea* cover when compared to the control, although biomass density in the 2000 inverted site was higher. The 2023 inverted site predominantly consisted of open water and high levels of dead *Molinea* due to the recent peat inversion so no conclusive results could be drawn from it. Hydrological data revealed stable water levels in both inverted sites, suggesting ideal conditions for *Sphagnum* recovery.

Ultimately, this research confirms that the monitoring of bog restoration efforts using drones and modern classification techniques can be accurate and effective. Thus, aiding in the improvement of restoration efforts to give the best opportunity for *Sphagnum* expansion and the return of peatland dynamics which are central in carbon sequestration and the continued provision of ecosystem services.

Keywords: Wetlands, Restoration, Bogs, Peat, Random Forest, Drone Survey, Classification, Peat Inversion, UAS, *Sphagnum*, *Molinea*

Glossary:

- **Acrotelm:** The upper layer of peat, consisting of partially decayed plant material that retains water.
- **Anaerobic Conditions:** Environments that lack oxygen.
- **Anthropogenic Climate Change:** Climate change driven or influenced by human activities.
- **Atmospheric Nitrogen Deposition:** The accumulation of nitrogen compounds in ecosystems from the atmosphere.
- **Biodiversity:** The variety of life forms within an ecosystem, including species richness and genetic diversity.
- **Bog:** A type of wetland characterized by acidic waters, peat accumulation, and specialized plant communities.
- **Carbon Sequestration:** The process through which carbon dioxide (CO₂) is captured and stored in biomass and soils, thereby reducing atmospheric carbon levels.
- **Carbon Sink:** A natural or artificial reservoir that absorbs and stores carbon from the atmosphere
- **Catotelm:** The lower layer of peat composed of more heavily decomposed plant matter, typically more stable and anaerobic.
- **Damming:** The construction of barriers in wetland areas to retain water and raise water tables.
- **Decomposition:** The biological process through which organic matter is broken down into simpler substances by microorganisms.
- **Ecosystem Engineer:** A species that significantly modifies its environment, thereby creating or maintaining habitats for other species.
- **Ecosystem Services:** The benefits that humans derive from ecosystems.
- **Eutrophication:** The process by which water bodies become enriched with nutrients.
- **Feedback Loops:** Processes in which the output of a system influences its own operation.
- **Hydrological Gradients:** Variations in water availability across a landscape.
- **Hydrology:** The study of water movement, distribution, and quality within ecosystems.
- **Microforms:** Specific small-scale landforms within bogs that create distinct habitats and affect water retention and plant communities.

- **Microtopography:** The small-scale variations in the surface elevation and features of an area, such as mounds and depressions.
- **Non-parametric Classifier:** A type of classifier that does not assume a specific distribution for the underlying data, allowing for greater flexibility in data analysis.
- **Nutrient Dynamics:** The movement and transformation of nutrients within an ecosystem
- **Peat Inversion:** A restoration technique that involves turning over the upper layer of soil.
- **Peat:** Accumulated organic material, primarily composed of decomposed plant matter, that forms in wetland environments under anaerobic conditions.
- **Random Forest Classification:** A machine learning algorithm that builds multiple decision trees to classify data based on various features.
- **Remote Sensing:** The use of satellite or aerial technologies to collect data about the Earth's surface.
- **Restoration Techniques:** Methods employed to rehabilitate degraded ecosystems.
- **Spatial Autocorrelation:** The degree to which a set of spatial data points correlates with each other, influencing the accuracy of statistical analyses.
- **Spectral Reflectance:** The amount of light reflected by a surface at different wavelengths, used in remote sensing to analyze vegetation types.
- **Tipping Points:** Critical thresholds at which a small change in environmental conditions can lead to significant and often irreversible changes in ecosystem structure and function.
- **Unmanned Aerial Systems (UAS):** Drones or aerial vehicles operated without a human pilot on board.
- **Vascular Plants:** Plants that have specialized structures (roots, stems, leaves) for transporting water and nutrients.
- **Wetlands:** Ecosystems characterized by high water levels, either permanently or seasonally, which supports aquatic and semi-aquatic vegetation.

Table of Contents

<i>Abstract</i>	2
<i>Glossary</i>	3
1. Introduction	7
1.1 Wetlands.....	7
1.2 Bogs & Peat Dynamics	8
1.3 Restoration	9
1.4 The Dutch Context	10
1.5 Remote Sensing.....	12
1.6 Random Forest Classification	12
1.7 Knowledge Gap & Aim.....	13
1.9 Hypothesis	14
2. Theory	15
2.1 Vegetation.....	15
2.2 Restoration	17
2.3 Remote Sensing.....	17
2.4 Random Forest Classification	19
3. Methods	21
3.1 The Study Area.....	21
3.2 Drone Survey	23
3.3 Ground Truthing Data.....	25
3.4 Pre-Processing of Drone Data	27
3.5 Vegetation Classification	30
3.6 Multispectral data	35
3.7 Hydrological Data.....	36
4. Results	37
4.1 The Random Forest Classification.....	38
4.2.The Multispectral data.....	46

4.3 Comparing Classification and NDVI.....	49
4.4.Hydrological data	50
5. <i>Discussion</i>	52
5.1.Random Forest classification	52
5.2.Analyses of the Multispectral Data	55
5.3.Hydrological data	56
5.4.Future research.....	57
6. <i>Conclusion</i>	58
7. <i>References</i>	60
8. <i>Acknowledgements</i>	70
9. <i>Appendix</i>	71
Appendix A- Final Map Rasters	72
Appendix 2- Precision and Recall for the classification tests	74

1. Introduction

1.1 Wetlands

Climate change represents an urgent and critical global issue, significantly impacting numerous ecosystems that provide essential ecosystem services (Salimi et al., 2021). The loss of these systems and their associated services has only recently come to the attention of the public and policymakers, making now an opportune moment to invest in conservation and restoration efforts to cease further losses (Antala et al., 2022; Salimi et al., 2021). Wetlands are one such unique ecosystem which provides vital ecosystem services, including water retention, climate regulation, flood control, recreation, and carbon sequestration (An & Verhoeven, 2019; Regan et al., 2019; Steenvoorden & Limpens, 2023a). Despite covering only 1-2% of the earth's surface, wetlands sequester over 20% of the global organic carbon (Müller & Joos, 2021; Steenvoorden et al., 2022; Temmink et al., 2022). Since the Industrial Revolution, 46% of global wetlands (Zou et al., 2022) and 21% of European wetland (Fluet-Chouinard et al., 2023) have been degraded due to drainage, deforestation, agriculture, urbanisation, and, most recently, anthropogenic climate change (Fluet-Chouinard et al., 2023; Green et al., 2017; Zou et al., 2022). Destruction and degradation of these systems have several negative environmental impacts, including increased wildfires in drained regions (Shepard et al., 2023), loss of biodiversity (Regan et al., 2019), reduced water retention exacerbating local flooding (Fluet-Chouinard et al., 2023), changes to regional microclimates, and a switch from carbon sinks to carbon sources (An & Verhoeven, 2019; Günther et al., 2020). Recent estimates indicate that approximately 276.4 +/- 175.5 Giga Tonnes of Carbon Dioxide (CO₂) have been released into the atmosphere from degraded wetlands over the past 71 years (Zou et al., 2022). These emissions contribute to climate change, leading to further degradation as higher temperatures dry out wetland areas (Green et al., 2017; Müller & Joos, 2021; Salimi et al., 2021). Thus, creating a positive (self-perpetuating) feedback loop: as peatlands dry, they release stored CO₂, accelerating global warming, further drying peatlands and releasing more CO₂ (Müller & Joos, 2021; Qiu et al., 2020). Every 100 Gt of Carbon released from peatlands could cause a warming of about 0.2 °C (Müller & Joos, 2021).

Bogs, a wetland subtype, exhibit resilience, typically withstanding various perturbations due to the interdependencies among wetland vegetation types, hydrology, topography, and climate, which collectively establish beneficial conditions like a high-water level and acidic pH (Dise, 2009; Steenvoorden & Limpens, 2023a). However ongoing climate stressors and land use changes are undermining these self-preserving dynamics and eroding this resilience

(Salimi et al., 2021). Continued disturbance could trigger tipping points, resulting in an abrupt transition of vegetation and ecosystems to a degraded state (Dise, 2009; Green et al., 2017; Müller & Joos, 2021). Projections indicate a decline in wetland areas, particularly bogs, across Western Europe due to climate change, with further warming potentially converting these areas to net carbon sources (Dise, 2009; Qiu et al., 2020).

1.2 Bogs & Peat Dynamics

Bogs are characterised by a high-water table, sustained by rainwater, and the accumulation of decay-resistant plant matter (Sahar et al., 2022). Resulting in a nutrient-poor but organic carbon-rich soil called peat, which grows and expands over millennia to form peatlands (Sahar et al., 2022). Anaerobic and low pH conditions within bogs inhibit decomposition, allowing the gradual build-up of organic material to form peat over extended periods (Shepard et al., 2023; Temmink et al., 2022; Treat et al., 2019). This results in high rates of carbon accumulation, leading to carbon densities of 1000-2000 MG C^{ha-1} (mega-grams of carbon per hectare) in peat (Temmink et al., 2022). Bogs support unique biodiversity, fostering specialised flora and fauna that contribute to peat formation and provide ecosystem services like carbon storage, flood control, water retention, and climate regulation (Bhatnagar et al., 2021; Regan et al., 2019). Bog plant types are organised along hydrological and topographical gradients, creating micro topographical features (microforms) (Sahar et al., 2022; Steenvoorden & Limpens, 2023a).

Three commonly occurring microforms in bogs include hummocks, lawns, and hollows. The vegetation type and associated microforms are strong indicators of peatland functions, as they 1) reflect hydro-physical properties like water flow and nutrient dynamics, 2) significantly influence carbon sequestration rates through the promotion of plant growth and decomposition, 3) maintain carbon sink function by encouraging plant diversity, and 4) enhance ecosystem resilience through reorganisation of plant types in response to changing precipitation and groundwater levels under climate change (Steenvoorden & Limpens, 2023a). The development and persistence of microforms are driven by feedback interactions between vegetation and abiotic factors (pH, light, water depth, nutrients, and temperature) (Steenvoorden et al., 2022; Temmink et al., 2022).

A key plant species in temperate bogs is peat moss (*Sphagnum*), which possesses self-regulating properties that enhance its environment, facilitating its survival and expansion by creating acidic, nutrient-poor, cold, and anoxic conditions (Lamers et al., 2000; van Breemen, 1995). *Sphagnum* plays a crucial role in microform development and influences the composition of co-existing plant species, as only certain species can co-exist in the acidic, waterlogged conditions it creates (Antala et al., 2022; van Breemen, 1995). Furthermore, *Sphagnum* is central to peat formation (Joosten, 1993), and the acrotelm, the uppermost layer of peat, is comprised of partially decayed plant material (Smolders et al., 2003). *Sphagnum* is highly sensitive to fluctuations in water level, expanding during periods of high water levels and compacting during low water conditions (Couwenberg & Joosten, 1999; Joosten, 1993). Extended periods of low water can lead to desiccation and death of *Sphagnum* patches, halting peat creation and carbon storage (Couwenberg & Joosten, 1999). Therefore, immediate and effective action is essential to ensure the protection of existing bogs and the restoration of degraded areas.

1.3 Restoration

Successful restoration of bogs hinges on the vegetation composition, which is central to peat formation and ecosystem resilience, but is facing increasing risks from land-use changes and increasing temperatures (Antala et al., 2022; Robroek et al., 2017). Bogs have been drying up for centuries due to drainage for peat extraction, agriculture, and urbanisation; the remaining areas are now under heightened pressure from climate change and nitrogen deposition (Müller & Joos, 2021; Steenvoorden et al., 2022). Drainage poses a particular threat to bogs, as it leads to peat compaction due to water removal, reducing the surface porosity and complicating recovery efforts (Joosten, 1993). The pore spaces which once reattained water become oxygenated, triggering aerobic decomposition of the organic carbon stored in the peat, which is subsequently released as carbon dioxide (Joosten, 1993; Jurasinski et al., 2020). Bog degradation has resulted in a loss of essential ecosystem services, and predictions indicate further increases in degradation if immediate action is not taken (Jurasinski et al., 2020; Müller & Joos, 2021; Salimi et al., 2021). Müller & Joos forecast a median loss of 61% for Northern peatland areas by 2300 under the most severe climate change scenarios, with even moderate scenarios predicting a median loss of 18% (Müller & Joos, 2021). These simulations link higher future emissions to increased loss of bogs, underscoring the urgent need for emissions reductions (Müller & Joos, 2021) and to conserve and restore bogs’

carbon-dense peat, which takes centuries to rebuild (Temmink et al., 2022). Restoring carbon sink capacity is a time-consuming process, and it may not return to previous levels, thus highlighting the necessity of protecting the remaining peatlands (Joosten, 1993; Loisel & Gallego-Sala, 2022).

Restoration efforts encompass a variety of techniques, the most common being rewetting (Renou-Wilson et al., 2019; Zou et al., 2022) This involves increasing an areas water table to encourage the reestablishment of bog plant species (Robroek et al., 2017; Smolders et al., 2002). Recently implemented strategies include soil inoculation, which entails the introduction of living matter from an intact target ecosystem to a degraded system, providing it with an intact microbial community and propagules for plant recovery (Shepard et al., 2023). Damming is often employed to maintain the raised water level after rewetting, dykes are installed in an area, and a window of opportunity is created for the recovery of bog species (Temmink et al., 2022). In Germany, an experimental study investigated the removal of the topsoil layer in a degraded bog prior to rewetting; this approach aimed to eliminate the previously cultivated vegetation and create more optimal conditions for bog plant species (Huth et al., 2022). Results demonstrated that topsoil removal caused a shift to a more nutrient-poor and acidic state, benefiting target species such as *Sphagnum* (Huth et al., 2022). A novel restoration technique is peat inversion, which involves flipping over the top layer of peat to disrupt the expansion of undesirable species, such as grasses which spread quickly and outcompete other plants, and facilitate the establishment of target plant types, including *Sphagnum* (de Bruin et al., 2023). Ongoing restoration efforts must be assessed and refined to enhance carbon sink capacity and bolster bogs' resilience to future disturbances (Loisel & Gallego-Sala, 2022). These restoration initiatives also represent a cost-effective and reliable mitigation strategy for policy makers (Qiu et al., 2020).

1.4 The Dutch Context

Historically, extensive areas of Northern Europe were covered in bogs; of the 59,372,700 ha, 46% have been degraded or destroyed (Hu et al., 2017; Jurasinski et al., 2020). In The Netherlands, approximately 180,000ha of bogs existed at the beginning of the 17th Century (Tomassen et al., 2010). However, centuries of drainage for agriculture have led to only isolated fragments (Brouns et al., 2016; Mathema, 2005; Quik et al., 2023). By 1900, only around 90,000ha remained, which declined to approximately 3,600ha today (Tomassen et al.,

2010). These areas are estimated to contain only 5ha of undisturbed, peat-forming raised bog (Tomassen et al., 2010). The remaining bog remnants are now exposed to elevated levels of atmospheric nitrogen deposition resulting from agricultural practices, primarily livestock farming (Andersen et al., 2017; Brouns et al., 2016; Mathema, 2005) and are increasingly threatened by drainage, pollution, and excavation (van Beek et al., 2023). Another issue is nitrogen and phosphorus from agricultural activities accumulating on the surface of the bog water, leading to eutrophication (Casparie, 1993) and algae growth (van Duinen et al., 2006).

One of the most significant remaining peatland remnants is the Fochteloërveen in Friesland, The Netherlands, which is recognised as a protected area under the European Union's Natura 2000 project (Quik et al., 2023). This region encompasses 1700ha of peatland with 50-200cm thick peat (Altenburg et al., 1993). This peat formed 6000-7000 years ago and remained largely untouched until the 16th Century, when minor peat extraction occurred, although it was not a significant fuel source at the time (Altenburg et al., 1993). However, considerable damage was caused in the 18th century when buckwheat was cultivated in the area, leading to the excavation of ditches and canals to drain the peat (Altenburg et al., 1993). The top layer was burned annually to create ash for fertilisation, resulting in nearly a meter of peat loss (Altenburg et al., 1993). The drying out and enrichment of the top layer has destroyed the acrotelm and facilitated the dominance of purple moor grass (*Molinea Caerulea*), whose deep roots allow access to the lowered water level, overshadowing and reducing the coverage of raised bog species, particularly *Sphagnum* (Altenburg et al., 1993; Smolders et al., 2002; Tomassen et al., 2010). The Fochteloërveen is managed by Natuurmonumenten, a Dutch conservation organisation focused on nature and biodiversity preservation (Altenburg et al., 2017). The management aims to maintain the open raised bog landscape and restore associated bog communities (Altenburg et al., 1993).

Restoration efforts in the area have included rewetting and damming to retain rainwater and sustain high water levels (Altenburg et al., 1993). To aid in rewetting the area, dams were constructed in two phases, 1982-84 and 1999-2002, this split the Fochteloërveen into first ten compartments and then forty (Altenburg et al., 1993; Mathema, 2005). This rewetting initiative aimed to encourage the spontaneous re-establishment of *Sphagnum*, which requires stable groundwater levels that are not too deep to permit light to penetrate and are maintained year-round (Mathema, 2005; Tomassen et al., 2010). The rewetting successfully raised the water level, however the problem of *Molinea* dominance persists in the area (Altenburg et al., 2017). Peat inversion was also implemented in sections of the Fochteloërveen, involving the

excavation and turnover of the top layer of peat to counteract the expansion of *Molinea* (de Bruin et al., 2023). This was carried out in 2000 and 2023 in separate sections. A study conducted in 2005 by Mathema noted a reduction in *Molinia* tussocks (an area of higher clumped grass) and an increase in *Sphagnum*-dominated patches (Mathema, 2005). It is unknown what the effect of this restoration is long-term.

1.5 Remote Sensing

Remote sensing is a valuable monitoring technique, allowing for the regular collection of detailed data over large areas (Bhatnagar et al., 2021). Traditionally, bog monitoring relied on in-field surveys, which were time-consuming, costly and often unable to cover the entire region due to uneven and waterlogged terrain (Jeziorska, 2019). Advances in remote sensing technology have improved the ability to survey across various landscapes, particularly bogs, allowing for rapid assessment of large areas and access to areas that are otherwise difficult to reach on foot (Guo et al., 2017; Jeziorska, 2019; Rasanen et al., 2020; Sahar et al., 2022). Unmanned aerial systems (UASs), such as drones, effectively capture the fine-scale heterogeneity of peat microforms and plant types (Bhatnagar et al., 2021; Jeziorska, 2019; Steenvoorden et al., 2023). Unlike traditional fieldwork, drone surveys do not disturb the delicate ecosystem, minimizing potential damage to plants (Beyer et al., 2019). Numerous studies have demonstrated the utility of drone surveying for wetland mapping, showing it to be time- and cost-effective for providing high-resolution images of vegetation types and distribution across small to large areas (Buznego, 2023; Diaz-Delgado et al., 2018; Guo et al., 2017). However, challenges remain, as drone operations are highly weather-dependent and cannot carry much weight (Bhatnagar et al., 2021; Guo et al., 2017; Jeziorska, 2019; Steenvoorden et al., 2023).

1.6 Random Forest Classification

The classification of ecosystems by plant type or functional group provides insights into their health, functionality, and utility (Antala et al., 2022; Simpson et al., 2024). In peatlands, the plant type and distribution can serve as indicators for monitoring biodiversity, carbon storage potential, ecosystem dynamics, and changes resulting from climate change, land use change

or hydrological fluctuations (Renou-Wilson et al., 2019; Simpson et al., 2024). Historically, classifying peatlands was labour-intensive, requiring in-field identification and documentation of individual plants (Bhatnagar et al., 2021; Steenvoorden & Limpens, 2023a). Data collected with drones can now be classified swiftly using publicly available platforms like ArcGIS (Bhatnagar et al., 2020). Over the last decade, several classification techniques have been developed and refined, leading to more accurate and efficient classifications (Amoakoh et al., 2021). The Random Forest method, an ensemble learning technique that utilises multiple algorithms to enhance prediction accuracy, has gained prominence in recent land cover classification studies (Berhane et al., 2018; Millard & Richardson, 2015). This method constructs multiple decision trees based on training data to determine the most likely class for a given area or object. Several studies have successfully employed Random Forest for wetland classification, yielding favourable results (Amoakoh et al., 2021; Berhane et al., 2018; Simpson et al., 2024). Classifying wetlands poses challenges due to their homogenous vegetation cover, requiring fine detail to differentiate features in satellite and drone images (Berhane et al., 2018; Simpson et al., 2024). Random Forest has outperformed other wetlands classification methods due to its ability to process large datasets and capture intricate details (Amoakoh et al., 2021; Berhane et al., 2018). There is an opportunity to integrate modern machine learning techniques, such as Random Forest, into the monitoring of restored bogs to streamline vegetation mapping and process data efficiently and accurately.

1.7 Knowledge Gap & Aim

Bogs are critical ecosystems that necessitate immediate attention to ensure their protection and restoration, thereby preserving essential ecosystem services (Salimi et al., 2021). Restoring specialised bog plant species, particularly *Sphagnum* mosses, is vital for reestablishing ecosystem health (Robroek et al., 2009; Smolders et al., 2002). Current restoration efforts often fail to achieve the desired outcomes in promoting *Sphagnum* expansion; therefore, innovative restoration methods must be implemented and monitored in the coming decades to evaluate their effectiveness (Crowley et al., 2021; Renou-Wilson et al., 2019). Using drones and classification tools can enhance monitoring efficiency, making it quicker, more affordable, and more precise (Bhatnagar et al., 2020; Steenvoorden & Limpens, 2023b). There is a current lack of research into the classification of plant cover in restored bog areas to assess the impacts of novel restoration strategies.

How do the restoration methods, specifically soil inversion, impact the cover of target species in the Fochteloërveen? To investigate this a drone surveying was combined with the Random Forest classification technique to compare two sites at a peatland remnant in The Fochteloërveen. These sites underwent a new soil inversion restoration technique in 2000 and 2023 to encourage *Sphagnum* expansion and reduce *Molinea* cover. The sites were compared to a control site to test the accuracy of the classification method, the cover of each plant type in the sites, how the plant biomass compares across the sites, how the hydrology of the sites has changed over the past decades and what impact this may have had on the vegetation, and finally did the peat inversion improve the cover of target species over the 20 years since its application.

1.9 Hypothesis

A drone survey and the Random Forest classification method are hypothesised to yield accurate study area plant-type classification maps. From these, it is hypothesised that the peat inversion restoration will have led to an increase in *Sphagnum* and a decrease in *Molinea* cover compared to the control area.

2. Theory

This section further explains the theoretical framework underlining this study, providing a comprehensive understanding of vegetation dynamics in bogs, restoration methodologies, and the application of remote sensing and modern classification techniques to facilitate the recovery of degraded bogs.

2.1 Vegetation

Current rates of climate change are unprecedented, representing the most accelerated environmental shift in the past 20 million years (Antala et al., 2022). Most European peat formed approximately 6000-8000 years ago and have never experienced environmental change of this magnitude (Antala et al., 2022; Casparie, 1993). These ecosystems exhibit limited capacity to adapt to such rapid alterations, resulting in a reduction in their functional services, particularly carbon sink capacity (Antala et al., 2022). Peat's high carbon accumulation potential depends on the presence of specialised plant species and specific habitat conditions- namely, a low pH and low nutrient and oxygen availability created by high water levels (Crowley et al., 2021; Schouwenaars & Gosen, 2007).

Water level and nutrient content fluctuate along topographical gradients, giving rise to the formation of unique habitats known as microforms within bog systems (Robroek et al., 2017; Steenvoorden et al., 2023; Steenvoorden & Limpens, 2023a). These microforms include hummocks, lawns, and hollows, as illustrated in Fig 1. Hummocks are typically associated with dry-adapted *Sphagnum* species, graminoids (grasses), lichens, and dwarf shrubs (Steenvoorden & Limpens, 2023a). Hollows exhibit a higher water table and are characterised by aquatic *Sphagnum* and occasional graminoids and sedges (Steenvoorden & Limpens, 2023a). Lawns represent the transitional area between hummocks and hollows, comprising more drought-adapted *Sphagnum* species (Schouwenaars & Gosen, 2007) and some graminoids, shrubs, and forbs (woody herbaceous plants) (Steenvoorden et al., 2022).

Sphagnum is an ecosystem engineer in bog ecosystems, facilitating the formation of these microforms (Steenvoorden et al., 2022). *Sphagnum* exhibits self-perpetuating dynamics by retaining moisture in an area and enhancing favourable conditions for its own growth (Steenvoorden et al., 2022; van Breemen, 1995). It can modify its environment to create wet,

acidic conditions advantageous to them but detrimental to other plants; consequently, only specific vascular plants, which have root systems adapted to waterlogged conditions, can coexist (Antala et al., 2022; Lamers et al., 2000). As a primitive plant devoid of roots or specialised water conducting tissue, *Sphagnum* is particularly sensitive to fluctuation in water levels (Antala et al., 2022). Nutrients are absorbed through the whole surface area of the moss, while water is taken in by capillary action (Antala et al., 2022). They are resilient plants once they have sufficient water and will continue to grow unless frozen (Antala et al., 2022).

Furthermore, *Sphagnum* is instrumental in the formation of the acrotelm, the spongy top layer of peat that retains water and protects the underlying catotelm layer, which consists of more heavily decomposed plant matter (Couwenberg & Joosten, 1999; Smolders et al., 2003). The acrotelm is a critical component of peatlands as it stores water and facilitates carbon retention by inhibiting decomposition (Smolders et al., 2003). Projections under climate change scenarios indicate a decline in *Sphagnum* populations and an increase in vascular plants in bogs due to temperature rises, reduced water availability, and more frequent drought events (Scholz & Salimi, 2021). This decline would adversely affect peat production, carbon storage, and water retention, all of which rely on *Sphagnum* (Schouwenaars & Gosen, 2007; van Breemen, 1995). Thus, fostering the resurgence and expansion of *Sphagnum* in degraded bogs is a key part of restoration efforts.

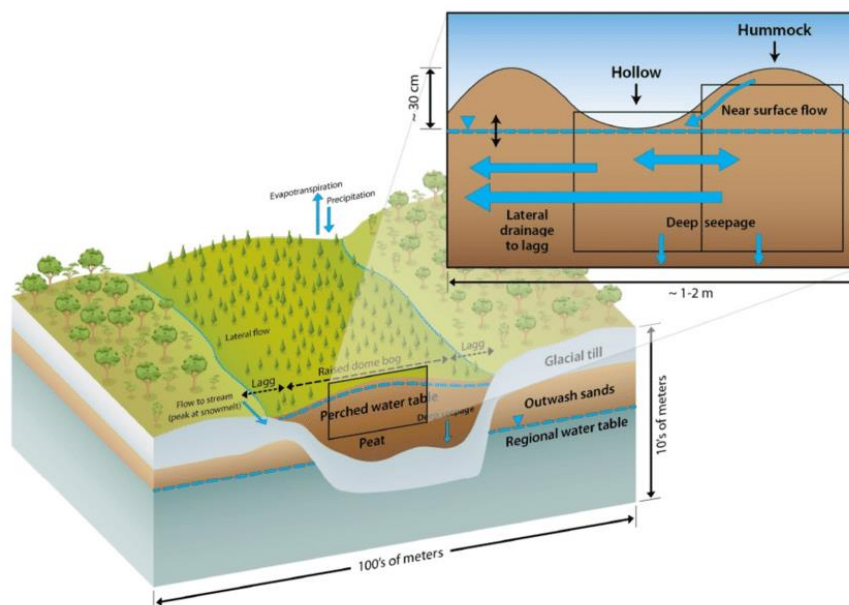


Fig 1. Conceptualisation of hummock and hollow microtopography (Shi et al., 2015)

2.2 Restoration

Conserving the remaining bog is imperative, as these ecosystems and associated services require centuries to develop and establish their interdependent dynamics (Loisel & Gallego-Sala, 2022; Salimi et al., 2021; Zou et al., 2022). In instances where bogs have been destroyed or degraded, restoration efforts such as rewetting, damming, soil inoculation, and peat inversion must be employed to restore natural ecosystem cycles and promote the return of typical bog plants and microforms (Loisel & Gallego-Sala, 2022; Zou et al., 2022). Current and historical restoration efforts have predominantly focussed on rewetting and maintaining high surface water levels to facilitate the return of peat-forming *Sphagnum* (Andersen et al., 2011; Robroek et al., 2009, 2017; van Duinen et al., 2006).

However, areas that have undergone rewetting alone have experienced stagnated recovery of target plant species (Rasanen et al., 2020; Robroek et al., 2017; Sahar et al., 2022). A comprehensive study of 71 peatlands in Germany that underwent rewetting found that typical peatland plants returned to only half of the sites, with some species remaining absent even after 30 years (Andersen et al., 2017). Conversely, other studies conducted in rewetted Irish bogs saw reduced short-term CO₂ emissions and predicted a long-term increase in carbon sequestration (Andersen et al., 2017). Notably, rewetting can also lead to short-term increases in methane emissions (Andersen et al., 2017; Jurasinski et al., 2020), particularly in the context of rising temperatures (Müller & Joos, 2021). Nevertheless, the long-term benefits of carbon sequestration and ecosystem restoration outweigh these temporary increased emissions (Günther et al., 2020)

European bog vegetation is characterised by a limited number of species with complex interrelationships and offers contrasting responses to climate change (Antala et al., 2022). Thus, restoring all relevant plant types is important for bog restoration and resilience (Antala et al., 2022). The presence of certain species and their abundance in the restored bog indicate the success of the restoration (Robroek et al., 2017; Simpson et al., 2024). Encouraging *Sphagnum* growth and expansion should be a priority, as it is an ecosystem engineer that sustains peat formation and system dynamics (Temmink et al., 2022; van Duinen et al., 2006). To ensure restoration work yields the desired environmental conditions, rigorous long-term monitoring is essential.

2.3 Remote Sensing

Remote sensing technologies, including drones, satellites, and sensors such as lidar, provide crucial data for monitoring bog health (Buchsteiner et al., 2023; Rasanen et al., 2020). They enable researchers to track vegetation types and ecosystem recovery across inaccessible or large bog areas (Steenvoorden et al., 2023). The presence of specific plant types serves as a strong signifier of ecosystem health and productivity; thus, monitoring these variables can quantify an area's recovery (Rasanen et al., 2019; Simpson et al., 2024; Steenvoorden et al., 2022, 2023). Recent advancements in remote sensing technology have enhanced the feasibility of vegetation classification and the monitoring of fine-scale objects (Bhatnagar et al., 2021).

Given that bog vegetation occurs at fine spatial scales, distinguishing and classifying them using satellite data is challenging (Diaz-Delgado et al., 2018; Steenvoorden & Limpens, 2023a). Satellite resolution is generally 10x10m (Bhatnagar et al., 2021), while peatland microforms and vegetation range from 0.1 to 1m (Steenvoorden et al., 2023), making it nearly impossible to capture them accurately. Drones are an effective intermediary between satellite surveying and manual field work, allowing for efficient coverage of large areas while capturing high-resolution images (Bhatnagar et al., 2021; Rasanen et al., 2019; Steenvoorden & Limpens, 2023a). The resolution of drones can have spatial resolution as low as 1.8cm, thus allowing for the easy capture of fine scale details (Bhatnagar et al., 2020). Modern drones can be outfitted with various sensors and scanners, including thermal, infrared, and laser-scanning capabilities, increasing their potential uses (Diaz-Delgado et al., 2018; Jeziorska, 2019). The resulting data can then be utilised to isolate the unique optical (spectral reflectance and colour) and structural (height and shape) features of individual plants or groups, facilitating identification during later analyses (Räsänen et al., 2019).

However, the size and weight of extra equipment is a limiting factor, as currently available drone models cannot carry excessive weight and are limited by battery capacity, necessitating frequent recharging for prolonged flights (Bhatnagar et al., 2021; Guo et al., 2017; Jeziorska, 2019). Furthermore, drones are also highly weather-dependent and cannot operate in windy conditions or capture accurate images during rain, mist, or snowfall (Bhatnagar et al., 2021; Guo et al., 2017; Jeziorska, 2019; Simpson et al., 2024). Additionally, variations in light and shadows in the study area can adversely affect the quality of images, leading to potential misclassifications (Buchsteiner et al., 2023). It is thus recommended that surveys be conducted at midday when the sun is at its highest to minimise the occurrence of shadows (Barbosa et al., 2019; Bhatnagar et al., 2021). Despite these limitations, drones represent an

ideal tool for rapid and cost-effective mapping of bogs, with many models capable of being pre-programmed with flight plans to optimise surveying efficiency (Jeziorska, 2019).

2.4 Random Forest Classification

Numerous classification methodologies have been employed to classify bog vegetation, including support vector machine learning (Amoakoh et al., 2021), K-nearest neighbour (Bhatnagar et al., 2020), maximum likelihood, and artificial neural networks (Berhane et al., 2018). Peatlands are characterised by high spatial heterogeneity and temporal hydraulic variability, rendering them among the most challenging ecosystems to classify (Berhane et al., 2018; Beyer et al., 2019). The diverse plant types are fine-scale and spectrally similar in drone images, complicating differentiation and classification (Steenvoorden et al., 2023). Recent studies have demonstrated that the automated image classifier, Random Forest, is an effective and accurate method (Bhatnagar et al., 2020; Rasanen et al., 2019; Steenvoorden et al., 2023) that reduces human error and facilitates the production of reproducible land cover maps (Amoakoh et al., 2021; Berhane et al., 2018). It has been used in several recent peatland vegetation and microforms classification studies, showing its accuracy even with such fine-scale data (Amoakoh et al., 2021; Berhane et al., 2018; Corcoran et al., 2013; Millard & Richardson, 2015; Steenvoorden & Limpens, 2023b)

The Random Forest algorithm is a machine learning approach that employs multiple classification trees, as illustrated in figure 2 below, and derives a final classification decision based on a majority vote (Badda et al., 2023; Berhane et al., 2018; Millard & Richardson, 2015; Räsänen et al., 2019). The classifier is trained on a sample set from the original dataset, which identifies unique spectral and spatial features of various classes (Millard & Richardson, 2015). The algorithm subsequently processes the original data, utilising the training data to allow each tree to determine the most probable class for each segment of the original dataset (Beyer et al., 2019).

Random Forest, a nonparametric classifier, is not limited by the distribution of predictor variables, allowing the use of randomised sample sets (Berhane et al., 2018). However, it is sensitive to the characteristics of the training data, such as sample size, class proportion, and spatial autocorrelation. Therefore, ensuring the data is high quality and accurate is important (Millard & Richardson, 2015). Ideally random samples would be used to better represent the proportion of each plant type in an area and to minimise human bias during data collection

(Millard & Richardson, 2015). That said, verifying random sample points can be challenging or impossible depending on the study area, so increasing the number of samples can help maintain classification accuracy (Millard & Richardson, 2015). The classifier is adaptable and can be customised to various classification requirements based on the input data and parameters (Badda et al., 2023). While Random Forest has been used effectively to classify healthy peatland areas, it has not been employed in restored regions to aid in monitoring and vegetation tracking.

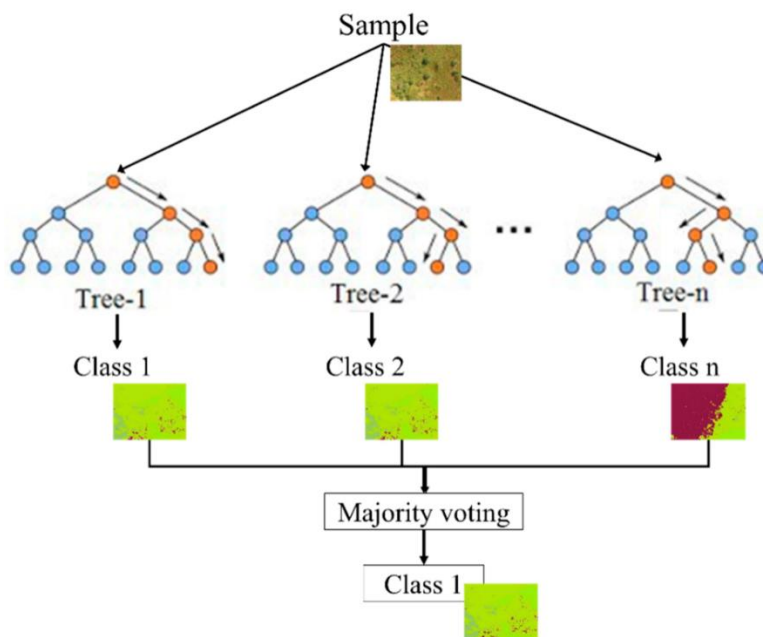


Fig 2. Workflow of the Random Forest classifier (Bhatnagar et al., 2020)

3. Methods

To answer the research question, a drone survey was conducted, after which the data was processed into maps using Metshape and then further processed in ArcGIS to prepare and optimise them for classification. The methods are based on several papers which undertook similar studies (Corcoran et al., 2013; Berhane et al., 2018; Beyer et al., 2019; Bhatnagar et al., 2020, 2021; Steenvoorden et al., 2023; Simpson et al., 2024) however, to simplify the process all processing, excluding creating the maps, was carried out on ArcGIS pro. Other studies used a few different platforms and alternative methods. Using one platform simplified and streamlined the process as ArcGIS had all the necessary tools required for the analyses.

3.1 The Study Area

The study was conducted in The Fochteloërveen, a bog remnant situated at the border between the provinces of Drenthe and Friesland in the north of the Netherlands (coordinates: 53.00443, 6.37070). It is the largest bog remnant, with 1700 ha, in the Netherlands and is representative of peatlands in the region, making it an ideal study area (Mathema, 2005; Quik et al., 2023; van Beek et al., 2023). Geographically it is located on the western edge of the Drenthe Plateau, which is underlain by glacial till deposits and aeolian cover sand (Altenburg et al., 1993; Quik et al., 2023). The average temperature in January is 5.2 C, while in July, it is 17.5 C. The area received an average annual rainfall of 837mm, with a potential evapotranspiration of 566mm recorded for 2023 (KNMI, 2024). A 50ha area of the Fochteloërveen was selected for the survey, this comprised three sites separated by dams.

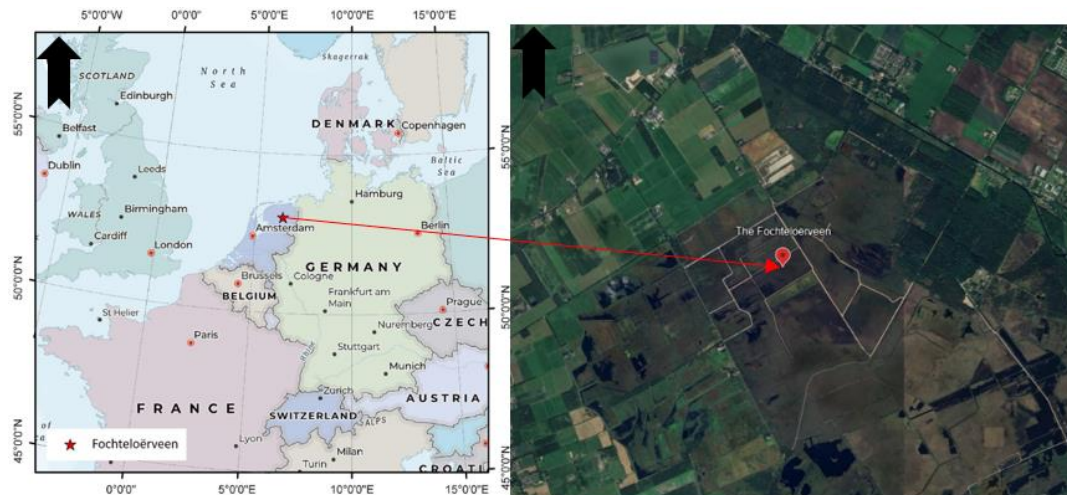


Fig 3. The Fochteloërveen, North Netherlands (van Beek et al., 2023) and Google earth, 2024.

Historically, the Fochteloërveen was utilised for buckwheat cultivation, which resulted in significant drainage and the excavation of deep ditches throughout the area (Altenburg). Coupled with the annual burning of the area for fertilisation, this has led to substantial loss of the upper peat layer, the acrotelm (Altenburg et al., 2017). Current vegetation cover in the study area is dominated by *Molinea Caerulea*, which poses a robust root system and rapid growth rate, thereby overshadowing and reducing the coverage of other plants, particularly *Sphagnum* (de Bruin et al., 2023). The presence of *Juncus effuses*, a type of rush, is attributed to agricultural phosphorus residue despite it being uncommon in the area (Andersen et al., 2017). Additionally, algae blooms have been observed around the periphery of each site, where the dams were installed in 1999, likely causing stagnation and nutrient enrichment from nitrogen and phosphorus runoff (Altenburg & van der Veen, 2003; van Duinen et al., 2006). Native plant species further include *Sphagnum* mosses, such as *S. magellanicum*, *S. papillosum*, and *S. rubellum*, as well as vascular plants typical of the ombrotrophic conditions, such as *Eriophorum vaginatum*, *Andromeda polifolia* and *Vaccinium oxycoccos* (Quik et al., 2023).

The Fochteloërveen also supports several protected bird and animal species, such as cranes and the large heath butterfly (Oosterwerld & van den Brink, 2010). The primary threats to conservation in the area originate from atmospheric nitrogen deposition and habitat desiccation due to the intense drainage (Quik et al., 2023). Restoration efforts undertaken by Natuurmonumenten aim to increase the coverage of *Sphagnum* species, such as *S. magellanicum*, *S. palustre*, or *S. rubellum*, to restore self-regulating dynamics within the

peatland (de Bruin et al., 2023). Previous interventions, including rewetting and damming, successfully raised the water level and increased the abundance of target species like *Sphagnum* (Altenburg et al., 2017). However, they failed to reduce the dominance of *Molinea* significantly (Altenburg & van der Veen, 2003; Jongman, 2021). Peat inversion has been implemented in specific sites of the Fochtelooërveen to try to reduce the *Molinea* coverage (de Bruin et al., 2023). This peat inversion work was conducted in 2000 on an 8-ha Site (Site A) and in 2023 on a 17-ha Site (Site B), as shown in figure 4 (de Bruin et al., 2023). A third Site (Site C) was used as a control area for comparative analyses. All three sites were part of a single compartment, divided in 1999 with the installation of wooden dams (Altenburg & van der Veen, 2003). The longevity of the wooden dams has been a concern for several years as leaks became more frequent (Altenburg et al., 2017), so currently, all dams at the Fochteleorveen are undergoing renewal to replace and reinforce them. A report from 2021 indicated an increase in *Sphagnum* cover to 25-50% in certain sampled plots since 2014, although *Molinea* cover remained high at 52% in most plots (Jongman, 2021).



Fig 4. soil inversion taking place in site B in 2023, photos by: J, de Bruin, 2023

3.2 Drone Survey

To investigate the three study sites, drone imagery was collected on March 6th, 2024. The DJI Phantom 4 multispectral drone was deployed over the sites and captured images in the visible red, green, and blue spectral bands, red-edge, and near-infrared (NIR) bands. The total area surveyed encompassed approximately 50 hectares. Prior to the flight, ground control point (GCP) markers, pictured in figure 5, were laid out at the four corners of the area, and four more were placed along the tracks between the sites (Simpson et al., 2024; Steenvoorden &

Limpens, 2023a). A Trimble global navigation satellite system (GNSS) was employed to obtain the precise Differential Global Positioning System (DGPS) coordinates and elevation for each of the eight markers.

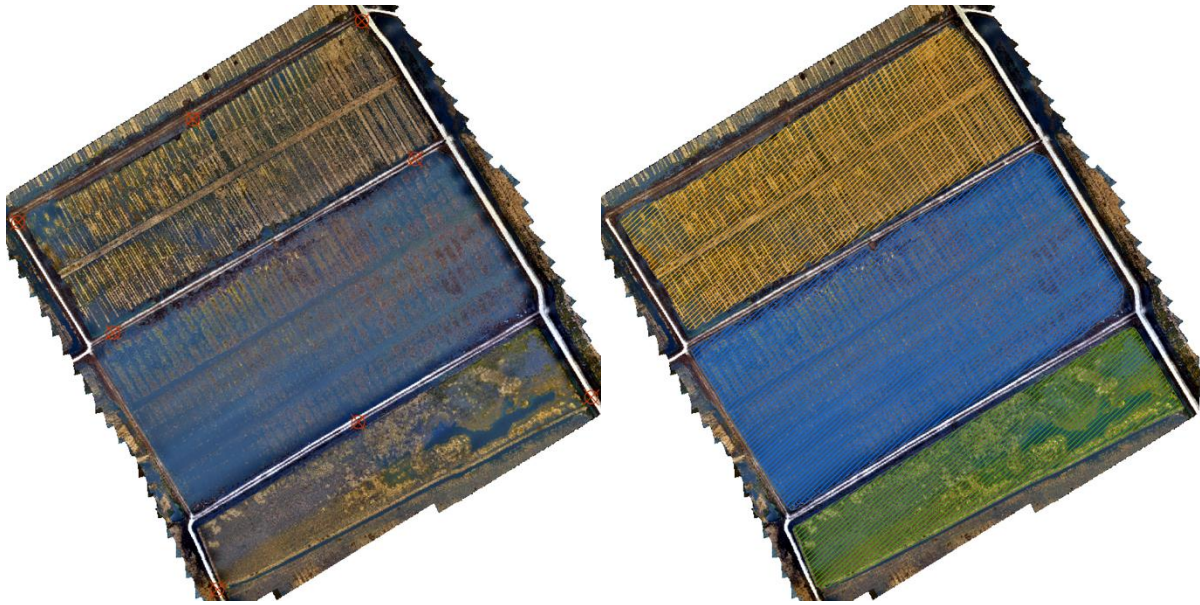


Fig 5. The ground control points are marked with red circles on the map (left) and the outlined sites (right). The site turned in 2000 (Green), the Site Turned in 2023 (Blue), and the Control Site C (Orange). Also, note the visible ditches and channels from the buckwheat cultivation in the 18th Century.

An automated flight plan was designed using the DJI Ground Station Pro before the survey, which was subsequently adjusted on the day of the flight to accommodate the large area and ensure sufficient detail was captured by reducing the flight speed. Prior to flight, the drone photographed the calibration reflectance panel, seen in figure 6. to later calibrate the images to the reflectance on the day. The survey took place in the morning on a clouded day to reduce shadows and reflection on the sites (Simpson et al., 2024). The drone was flown at an altitude of 50 meters above ground level (approximately 62m Normaal Amsterdams Peil, NAP, elevation), with a 75% frontal and a 60% side overlap (Steenvoorden et al., 2023). The drone was stopped periodically to change the battery; in total, eight were used. During this flight, RTK (real-time kinetic positioning) was employed to correct common errors in the satellite positioning. The location data for the final images were highly accurate, with a theoretical max error for this flight was X:1.3 cm, Y:2.0cm, Z:3.2cm. The data was collected in the Rijksdriehoeksmeting Normaal Amsterdams Peil (RDNAP2018) geodata reference system, which is the standard Dutch national system.

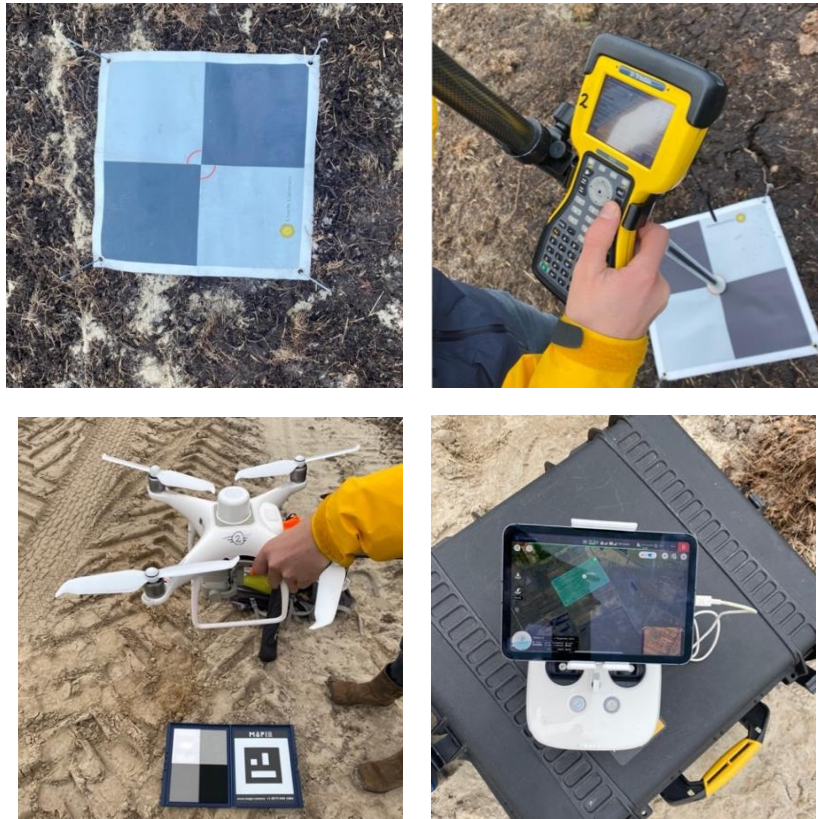


Fig 6. A Ground control marker (top left) and Trimble GNSS system (top right) DJI Phantom 4 multispectral drone with calibration reflectance panel (bottom left) and control panel (bottom right) showing a section of the flight plan, Photos by J. O'Donovan.

3.3 Ground Truthing Data

To create the training samples for classification (Simpson et al., 2024), ground truthing data was collected on March 11th, 2024. This took place as close to the time of the drone survey as possible to ensure samples could accurately be matched to the drone images. Samples were taken of ten different plant types- *Sphagnum* ($n = 26$), *Molinea* ($n = 18$), *Juncus* grass ($n = 15$), Bare peat ($n = 17$), Open water ($n = 18$), Algae ($n = 5$), Heather ($n = 10$), Cranberry ($n = 3$), Dead *Molinea* ($n = 9$) and examples of mixed areas- *Molinea/Sphagnum* ($n = 5$) and heather/ *Sphagnum* ($n = 3$), pictured in figure 7 below. A hand-held Garmin GPS was used to record the coordinates, while the coordinate ID name and the corresponding plant type for

each were noted in a waterproof notebook. Additionally, a waterproof camera was used to take pictures of representative plots.



Patch of Peat Moss



Purple Moor Grass



Open water



Bare peat



Algae



Juncus grass



Heather



Cranberry

Fig 7. The 8 Classes of vegetation collected during the fieldwork, Photos by R, Temmink, 2024.

Where feasible, a target of 15 samples was taken for each class, although some classes, such as cranberry, were under-sampled due to sparse coverage and inaccessible areas. Due to these

accessibility challenges from uneven terrain and high-water levels, the majority of samples were collected from the edge of the Sites, as shown in figure 8.



Fig 8. showing inaccessible conditions in Site B (left), Photo by: R, Temmink 2024, and map of sample points, ArcGIS 2024.

3.4 Pre-Processing of Drone Data

Creation of orthomosaic maps in Metashape

In total, the drone captured 3,386 images for the Red, Green, and Blue (RGB) spectrum and 16,970 for the Multispectral (MS) spectrum. Due to the extensive size of the data, a high-powered processor was required to generate the orthomosaic raster layer. The term ‘orthomosaic’ refers to a comprehensive image constructed from multiple images, while a ‘raster layer’ denotes a grid of pixels organised into rows and columns, which can be processed and analysed in ArcGIS and other mapping platforms (ERSI, 2024). An Earth Simulations Lab (ESL, Utrecht University) technician was engaged in constructing the orthomosaiced raster layers as neither a standard laptop nor the university computers had the requisite processing capacity. The drone images were uploaded to Agisoft Metashape, where the cameras were aligned. Points that did not appear in more than two drone images, had too high a reconstruction uncertainty (10+), or a reprojection error of 0.5+ were removed. Camera optimisation was run between these checks to ensure optimal quality. A point cloud was generated, with all the points exhibiting a confidence of 5 and lower being removed. A

point cloud is a set of data points in a 3D coordinate system. A Digital Elevation Map (DEM) was generated with thorough filtering to remove any floating points, providing topographical information for the area (Steenvoorden et al., 2023). Subsequently, orthomosaic maps were created based on the DEM for both the MS and RGB datasets. The RGB raster consisted of three spectral bands, which produce images within the visible spectrum, while the MS raster included five bands (Red, Green, Blue, red-edge, and Near Infrared (NIR)). All maps had a resolution of 5cm.

Alignment and defining of maps in ArcGIS Pro

The maps were imported into ArcGIS Pro (Buchsteiner et al., 2023) with the coordinate system set to Rijksdriehoeksmeting Normaal Amsterdams Peil (RDNAP2018). The following three steps were taken:

1. Ground Control Points (GCPs)

GCPs ensured that the processed maps contained reference points with known coordinates, thereby facilitating alignment with the study area (Simpson et al., 2024; Steenvoorden et al., 2023). The GCPs were added to the raster layer by manually locating the ground control markers on the image and assigning the corresponding coordinates to each. These were then saved, and the map was adjusted to align the GCPs with their GPS coordinates (Bhatnagar et al., 2021; Buchsteiner et al., 2023; Simpson et al., 2024).

2. Site definition

A shapefile of each site was created to delineate them for later analyses. Shapefiles are vector data storage formats that store geographic features, such as location, shape, and attributes. A polygon shapefile was used to differentiate the sites, shown in figure 9. A comprehensive shapefile was also generated to encompass all three sites and exclude 12,6 metres surrounding the dams at the site borders to remove the road and unwanted sites. This shapefile was used to clip the rasters to the correct size for classification, so only the target areas were classified. The site shapefiles were later revised to exclude marginal areas around each site due to certain classes being removed.

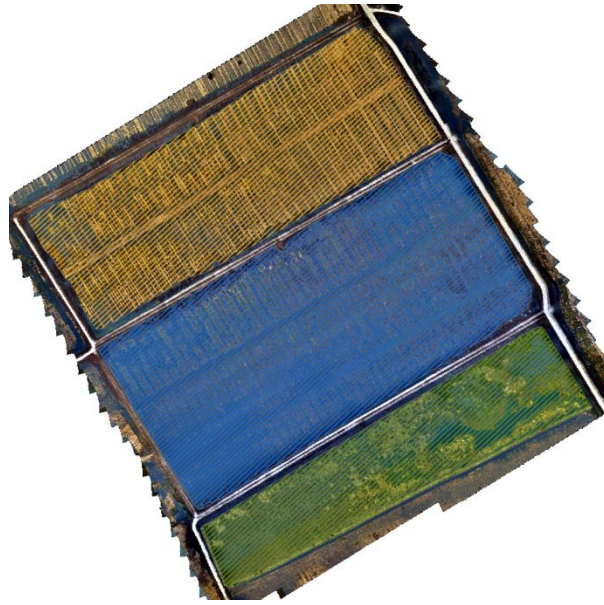


Fig 9. The shape files that defined each site, 2000 inverted site (green, 2023 inverted site (blue), and control site (orange).

3. Clipping & segmenting

The RGB raster was clipped using the previously made shapefile to encompass just the three sites. The segment mean shift tool was then used to group pixels into objects and regions based on similar spatial and spectral characteristics (Dronova, 2015; Steenvoorden et al., 2023). This pre-processing step was performed to enhance processing efficiency during classification. Spectral detail was prioritised by setting the parameter to the highest value (20), enabling improved differentiation of spectrally similar features. The spatial detail parameter was similarly set to 20, given the small and clustered nature of the features of interest. The minimum segment size was set to 1 to preserve detail for training samples and classification (Steenvoorden et al., 2023), as shown in figure 10.

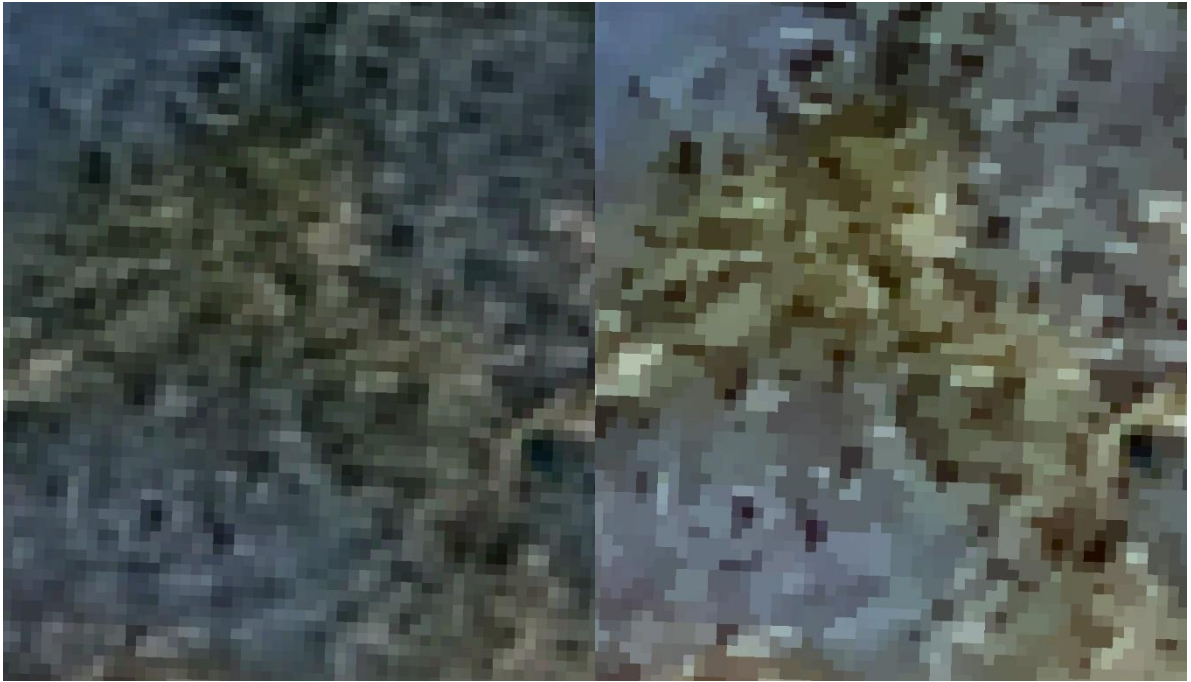


Fig 10. Section of Site A before segmenting (left) and after (right).

3.5 Vegetation Classification

Organising the data

The collected ground truthing data were organised by uploading the coordinates to Garmin Base camp, converting them to a CVS file and then adding this to an Excel sheet. Each coordinate was matched to its corresponding class type based on the field notes, and the Excel file was imported into ArcGIS, converting the data into point features using the table-to-point tool. The sample manager tool was utilised to create a classification schema of the collected classes. A 1x1m square grid was overlaid on the raster layer, and square polygons of 1m² were manually drawn around each sample point to add it to the correct class (Amoakoh et al., 2021, Steenvoorden & Limpens, 2023), as shown in figure 11. Some points were not precisely aligned with the correct class due to accessibility issues or human error, so some polygons were placed on the nearest correct class, as shown in Figure 11.

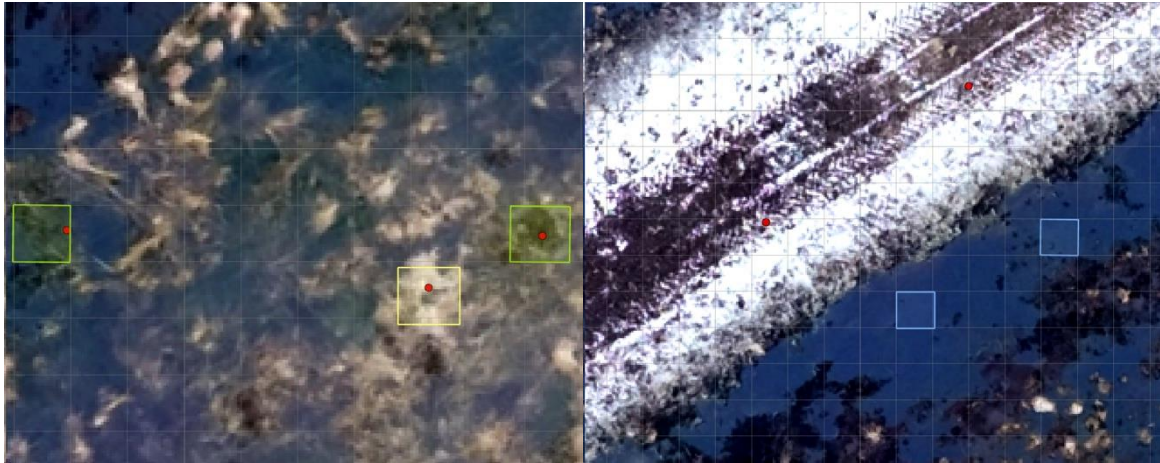


Fig 11.. 1x1m Polygons were drawn around the samples collected during fieldwork (left). Some points were not directly over the correct class, so the nearest correct area was used (right).

A training sample set was generated from the ground truthing data and processed through the classification wizard tool in ArcGIS, utilising the RF classifier with default setting (50 trees, 30 tree depth, max 1000 samples). Each tree within the classifier used the training data to predict the most probable plant class, with the most frequently predicted class being assigned to each object (Millard & Richardson, 2015). The number of trees influences the final classification decisions, with an average of all the decisions taken as the definitive classification. The tree depth determines the branching complexity, with more branches allowing for a greater variety of outcomes; however, given the limited number of outcome classes in this study, a high depth was deemed unnecessary.

The initial classification results indicated considerable confusion between visually similar classes, such as algae and submerged *Sphagnum*, as well as *Juncus* and elevated *Sphagnum* patches. After the dams' creation, increased nutrient levels at the site's edges led to sporadic algae blooms and *Juncus* patches, as shown in figure 12 below. Due to this, the site shapefiles were revised to exclude 3-4m around each site to remove these misclassification issues from the results. After revising the sites, algae and *Juncus* were removed as classes as they were no longer relevant. Classes with insufficient sample points, such as *Sphagnum*/Heather and *Molinea*/*Sphagnum*, were also removed.

Additionally, a new class was created for submerged *Molinea* grass, which was visually distinct from standard *Molinea* patches but had not been sampled in the field. Samples were identified in the drone imagery and added to the training sample data. Cotton grass was

similarly added as a class as it is significant in the study area but grows deeper in the sites and was overlooked during fieldwork. Instances of cotton grass were identified from drone imagery based on their prominent yellow flowers and corroborated with a 2020 vegetation analysis of the area (Jongman, 2021). Cranberry and heather were grouped into a single shrub class as they were visually similar and belonged to the same plant family, Ericaceae.



Fig 12. Algae (turquoise areas in the water) and *Juncus* (dark green patches) are growing around the edges of the Control Site (top left) and the 2000 inverted Site (top right). Picture Cotton Grass with distinctive yellow flowers (bottom left) (J.O'donovan, 2024) and water/*Molinea* class in the 2000 inverted site (bottom right).

Reducing the number of samples enhances the accuracy of the classifier and diminishes visual confusion (Badda et al., 2023; Berhane et al., 2018; Dronova, 2015), thus the final number of classes was condensed to Eight: ***Sphagnum*, *Molinea*, Open Water, Peat, Cotton Grass, Dead *Molinea*, Shrubs, and Open Water/*Molinea*.**

Creating training samples reference samples

Different training sample sets were created with 25, 50, 75, and 100 samples per class (Millard & Richardson, 2015). The original field samples were retained for reference data. Further samples of each class were identified manually in the drone images from areas close to the original data. Each sample set was processed through the classification wizard on ArcGIS Pro using the Random Forest classification with the default settings (50 trees, 30 depth) to facilitate accurate comparison. Some classes, like shrubs, cotton grass, and dead

Molinea, were less common in the sites, complicating the identification of more samples as the sample set size increased. Incorporating more samples improved the classifier's accuracy when comparing the classified layer to the original RGB image. Ultimately, a sample set of 80 samples per class was determined to be optimal, resulting in a total of 640 samples being used to train the classifier. This sampling strategy may not accurately reflect the field proportions of each class, as certain classes, like shrubs, were only sporadically observed, while others, such as open water, were more prevalent throughout the study area. Given the uncertainty surrounding exact class proportions in the field, an equal number of samples per class was selected to avoid overrepresentation, albeit this approach could result in the overclassification of less common classes (Millard & Richardson, 2015).

A reference sample set was created using the original field data and consisted of 160 separate samples, 20 per class. These samples were not included in the training sample set, thus enabling a more accurate evaluation of the classifier's performance. A confusion matrix was generated following each classification run (Dronova, 2015; Tian et al., 2016), illustrating the agreement between the classified and reference datasets through binary classification, as depicted in figure 13. The matrix calculated the ratios of true positives (TP), false positives (FP), true negatives (TN), and false negatives (FN). High TP and TN rates characterise an effective model alongside low FP and FN rates (Suresh, 2020). Metrics such as precision (the proportion of accurate positive predictions among all positive predictions) and recall (the proportion of true positive predictions relative to all class instances) were derived from the confusion matrix (Buchsteiner et al., 2023; Steenvoorden & Limpens, 2023a). The F1 score was also computed, which evaluates the balance between precision and recall. An F1 score of 1 indicates perfect predictions, while scores ranging from 0 to 100 reflect the likelihood of correct classifications (Steenvoorden et al., 2023, Buchsteiner et al., 2023). In conjunction with overall accuracy scores, these metrics facilitated the evaluation and comparison of different tests to determine the most effective classification methodology.

		Predicted	
		Negative (N) -	Positive (P) +
Actual	Negative -	True Negative (TN)	False Positive (FP) Type I Error
	Positive +	False Negative (FN) Type II Error	True Positive (TP)

Fig 13. Confusion matrices binary classification, (Suresh, 2020)

Testing the classifier

To ascertain the optimal inputs and parameters for the Random Forest classifier, a series of tests were conducted using the finalised training sample set and reference dataset (Amoakoh et al., 2021; Bhatnagar et al., 2021; Millard & Richardson, 2015; Steenvoorden et al., 2023). Each test was done four times to ensure reliability, and the average results were computed in Excel to account for any variability across the runs. The evaluation metrics of accuracy, precision, recall, and F1 scores were calculated for each test and subsequently compared to establish which inputs and parameter values yield the most accurate classification.

Layer combinations: To improve the classification, the RGB raster layer was combined with additional raster's that contained topographical data (DEM raster) and plant biomass data (normalised difference vegetation index -NDVI raster) (Amoakoh et al., 2021; Corcoran et al., 2013). NDVI is explained further below in the multispectral data section. These combination rasters provided the classifier with more distinctive information on each object for differentiation (Amoakoh et al., 2021; Dronova, 2015). First, the DEM and NDVI rasters were resampled, Using the 'resample' tool to ensure they had the same spatial resolution and could be combined without issue (Corcoran et al., 2013). The layers were combined using the 'Combine Bands' tool in ArcGIS. The classification was run with the RGB data, then the RGB combined with the DEM data, the RGB combined with the NDVI data and finally, all three layers combined. Each raster was clipped to the dimensions of the study area and segmented into objects. The default Random Forest setting (50 trees, 30 depth) was used for classification. The configuration yielding the most accurate results was then used for the subsequent analyses.

Further optimisation of the Random Forest classifier was achieved by varying the number of trees used in the classification parameters (Beyer et al, 2018). Tests were run using the

following tree counts: 50, 100, 200, 300, and 400 while maintaining the tree depth at the default setting of 30. Additionally, the impact of tree depth on classification accuracy was assessed by running the classifier with a fixed number of trees (50) while varying the depths to 20, 30, and 40.

To improve the differentiation among objects within the RGB imagery, a colour enhancement technique was employed using the stretch function in ArcGIS. The sigmoid stretch method emphasises moderate pixel values while preserving contrast between extreme values. This reduces contrast in very bright or dark areas while enhancing contrast in more homogeneous regions. Strength levels 1 and 2 were tested as going higher caused the classifier to malfunction. Additionally, the Minimum- Maximum stretch was also tested; this distributes the pixel values of a raster across the image's range of values, brightening and increasing the image's contrast, resulting in more distinguishable features. Each stretch was applied to the RGB raster using the stretch function available in the raster functions tab, resulting in a new raster that was then combined with the DEM and NDVI rasters as determined by the earlier combination tests. The combination raster was then clipped to the appropriate size and classified using the default Random Forest parameters.

Final process

The results of the tests were analysed by comparing the overall accuracy of each test using a confusion matrix. The most accurate result from each was used in the finalised set of inputs and parameters for the classification. To ensure consistent results, the classifier was run four times to compare the precision, recall, F1 score, and class cover. The class cover statistics for each Site were taken from the classified layers using the zonal statistics to the table tool and copied into Excel. The percentage covered by each class was calculated per site, and the results were compared, first to a 2020 vegetation survey (Jongman, 2021) of the study area to assess changes and then between each site to compare coverage.

3.6 Multispectral data

A normalised difference vegetation index (NDVI) raster layer was generated to analyse the multispectral data (Amoakoh et al., 2021; Berhane et al., 2018; Tian et al., 2016). NDVI serves as an indicator of vegetation presence and health across an area, allowing for comparison between the restored sites and the control. Robust and abundant vegetation

reflects strongly, yielding high positive NDVI values, while sparse or stressed vegetation results in lower values (Berhane et al., 2018, Tian et al., 2016). Water bodies are assigned negative NDVI values, while bare soil and ground typically yield values near zero (Berhane et al., 2018). The NDVI is calculated using the formula: $(\text{NIR} - \text{R}) / (\text{NIR} + \text{R})$, where NIR denotes near-infrared reflectance and R represents red reflectance. The resulting raster layer assigns a value ranging from -1 to 1 to each pixel, indicating vegetation health, with 1 representing maximum productivity and -1 indicating inactivity. The NDVI layer was subsequently clipped to the dimensions of each site and reclassified using the reclassify tool to establish six categories denoting various levels of vegetation densities:

1. -1 to 0.2: None
2. 0.21 to 0.4: Low
3. 0.41 to 0.6: Medium
4. 0.61 to 0.8: High
5. 0.81 to 1: Very high

The statistics for each Site were extracted using the zonal statistics to table tool and uploaded to Excel to calculate the area covered by each productivity level for comparative analyses.

3.7 Hydrological Data

Water level is a critical factor influencing bog development and plant community composition, particularly *Sphagnum*. Consequently, hydrological data from the study area were analysed to assess their potential impact on vegetation growth. Groundwater and surface water level data were recorded by automated measurement stations and accessed via the water web database. The data was organized in Excel, structured by month and year using pivot tables, and comparisons were made across the three sites to elucidate potential correlations between water levels and vegetation development. The data covered the period from 2000 to 2022 for the 2000 inverted site and the control site, however the measuring station for the 2023 inverted was only installed after the inversion so the data only covered November 2023 to March 2024.

Initially, the three sites operated as a single compartment, which was subsequently divided through the installation of wooden dams in 1999 (Altenburg et al., 2003). Data from older,

non-operational stations was also reviewed to compare pre-damming water levels with those measured post-installation. This covered the period from 1985 to 2000.

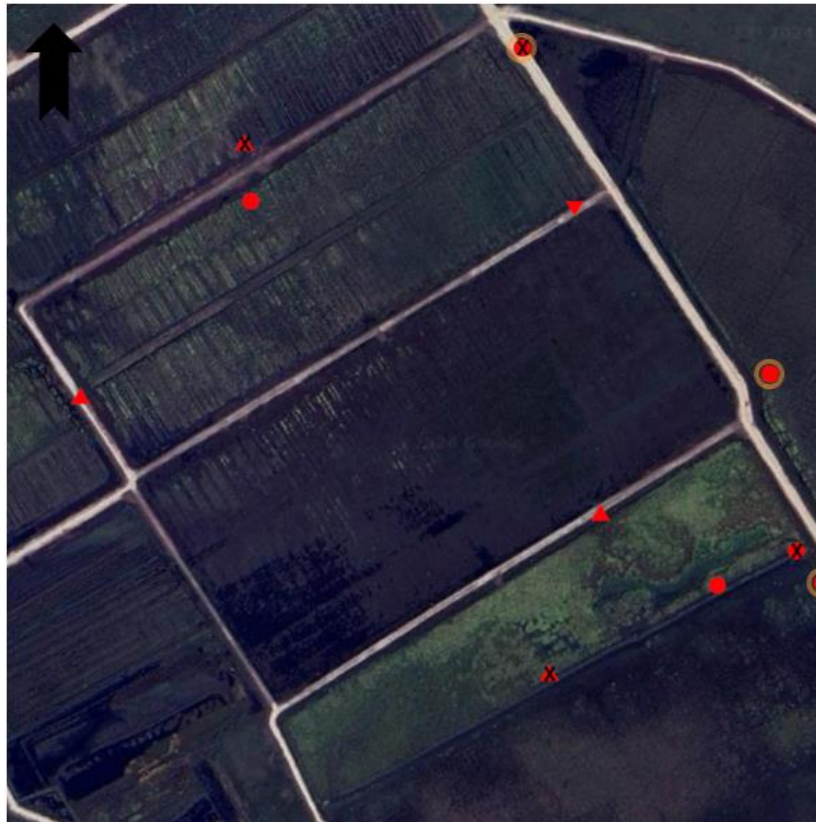


Fig 14. The study area with the groundwater measurement station marked by red circles, surface water measurement stations marked by red triangles, and stations marked with a black X no longer operate but contain historical data on the Sites.

4. Results

The results of the analyses are presented below, first the conclusion from the Random Forest classification tests will be laid out, along with the accuracy figures and class coverage of the final classification process. Then the multispectral data analyses will be presented and finally the hydrological data.

4.1 The Random Forest Classification

The results of the various tests on the inputs and parameters for the random forest classifier are summarised as follows:

The combination raster had a notable increase in overall classification accuracy as shown in figure 15. below. The RGB image alone had an overall accuracy of 75% which dropped to 74% with the addition of the DEM. The combination of RGB & NDVI achieved an overall accuracy of 77% while the combination of all three layers yielded the highest accuracy of 87%. This raster was subsequently used for the remaining tests. The results are present in figure 16 below where a sample from each site is presented to visually compare the various combinations. The addition of the DEM aided in differentiating areas of different elevation, while the NDVI caused green areas more to be more accurately classified. The control site saw the least drastic changes over the combination tests while the two inverted sites had clear classification changes.

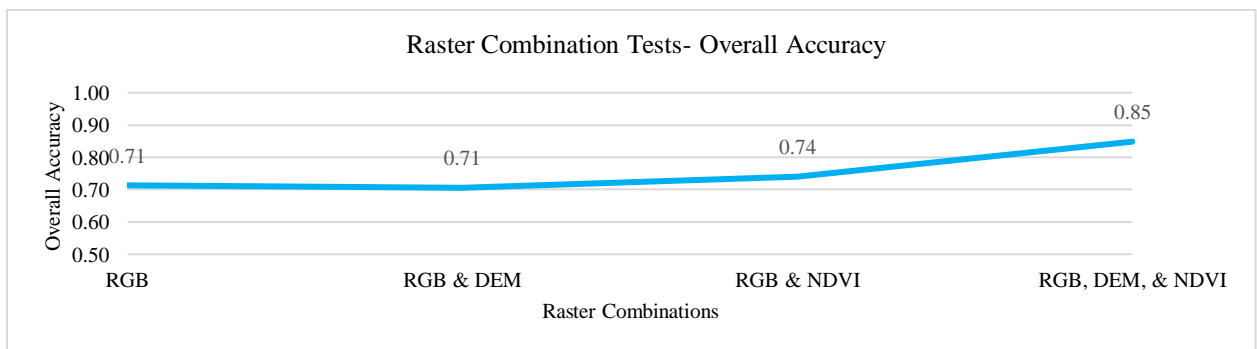


Fig 15. Overall accuracy for the raster combination tests.

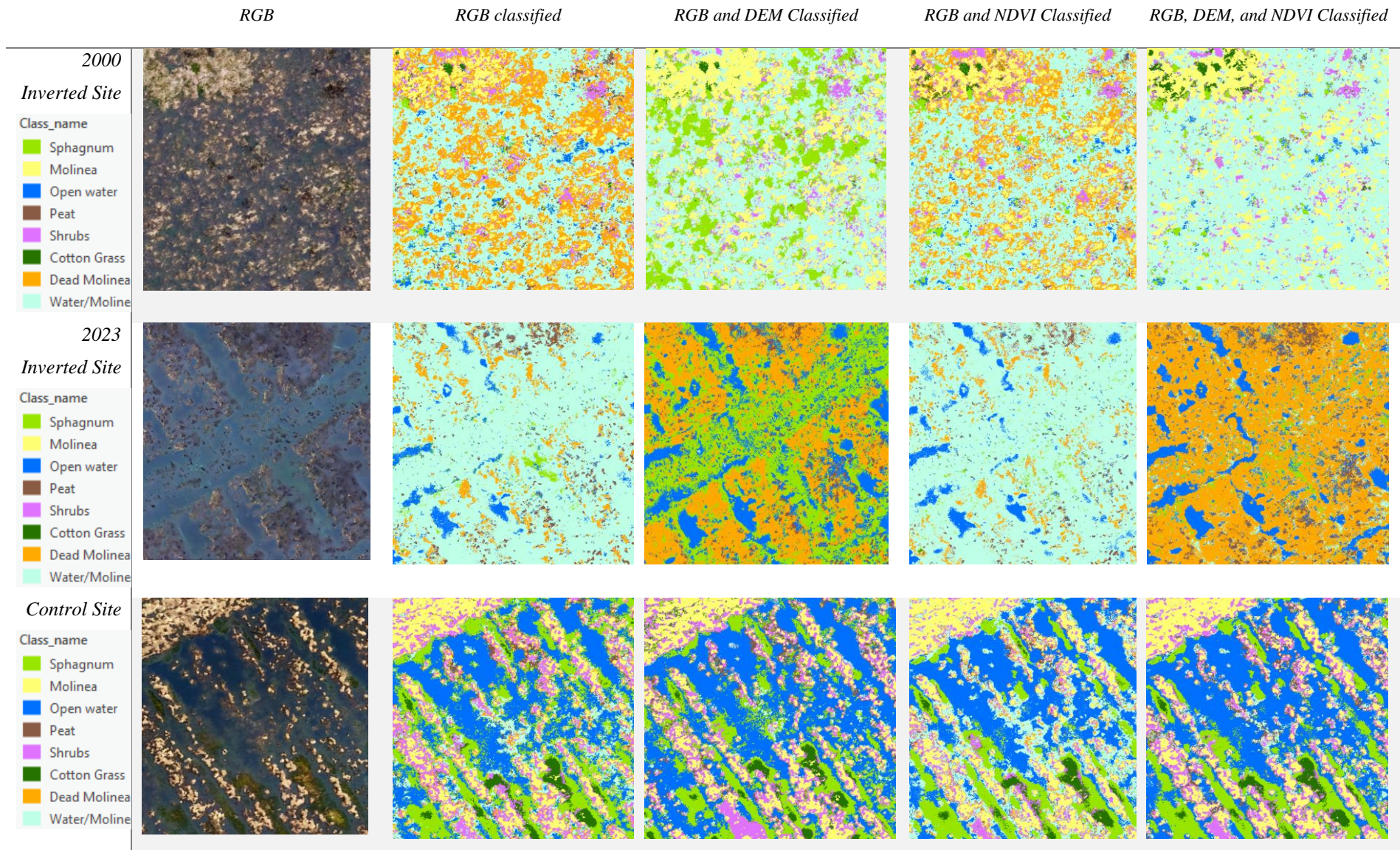


Fig 16. Raster combination tests , showing the RGB image and the classified RGB , RGB and DEM, RGB and NDVI, and RGB, DEM, and NDVI

The Random Forest number of trees tests demonstrated consistent overall accuracy across all variables, with the lowest accuracy being 85% with 300 trees and the highest being 87% for both 50 and 400 trees. The Random Forest tree depth variables also exhibited similar overall accuracy, with depths 10 and 40 having the lowest accuracy of 85% and depths 20 and 30 having the highest at 87%. The stretch tests yielded equivalent overall accuracy for both the sigmoid level one and level two tests at 87%, while the minimum-maximum stretch was marginally higher at 88%.

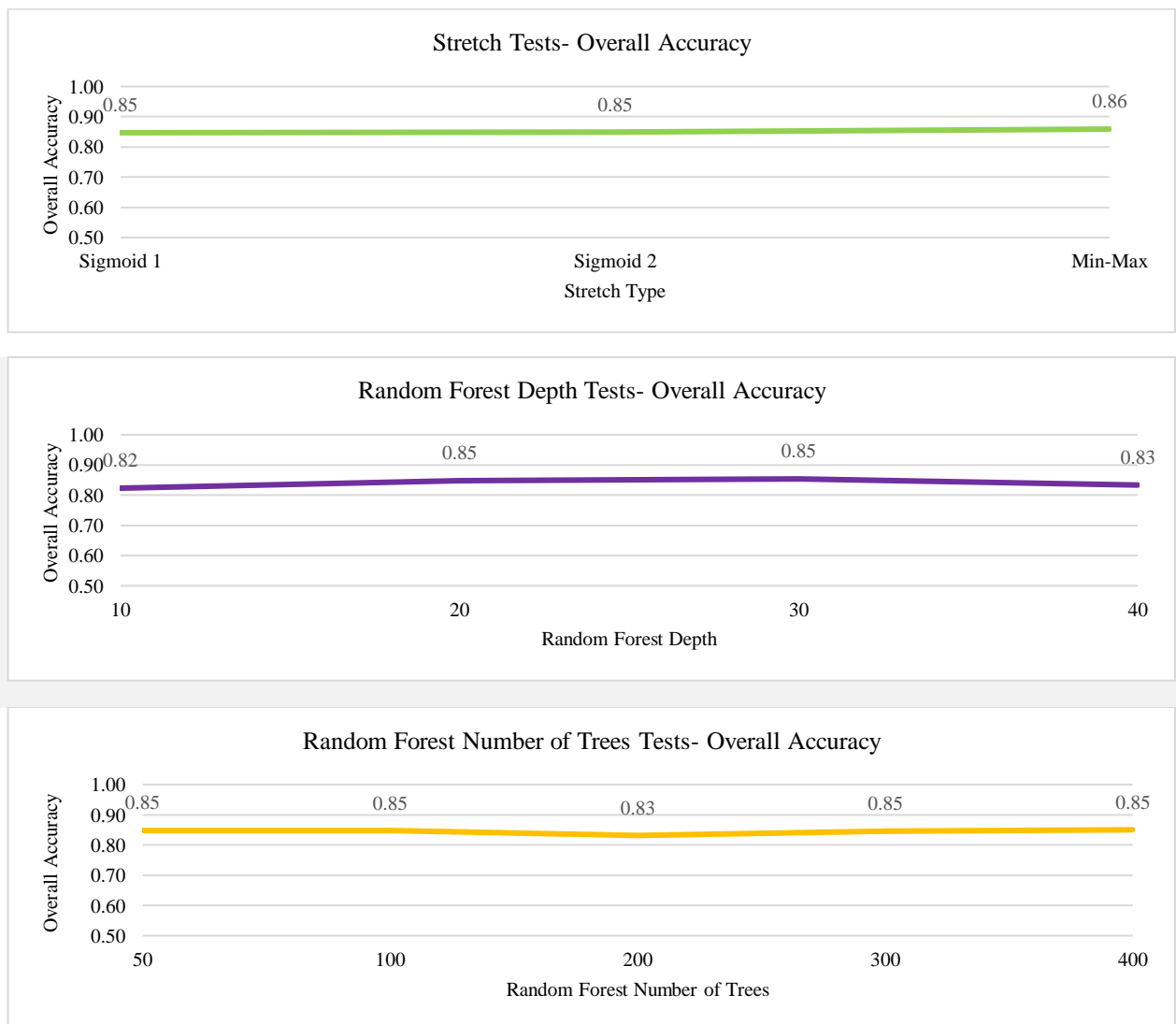


Fig 17. The overall accuracy for each variable in the Stretch, Random Forest number of tree, and Random forest Depth tests. .

Final classification

Based on the results of the tests, the optimal raster for the classification was determined to be the combination of RGB, DEM and NDVI, with the contrast of the RGB raster enhanced using the minimum-maximum stretch prior to combining. The optimal parameters for the Random Forest classifier were determined to be 50 trees and a tree depth of 30. These inputs were run several times to ensure consistency.

Figure 18 below shows the Minimum- Maximum stretch applied to the RGB raster, thus increasing the contrast. Yellow and green areas appear brighter and easier to distinguish from one another. The water also appears brighter, however, in Site B, it better highlighted the submerged peat in the water, which caused some misclassification.



Fig 18. Section of Site C showing how the Minimum- Maximum stretch 2 increased the contrast of the RGB image (left).

The final classification achieved a high accuracy of 88%, effectively differentiating between the finer details. In the 2000 inverted site, the classifier successfully separated patches of floating and submerged *Sphagnum* from the mass of vegetation. In the 2023 inverted site the classifier accurately delineated areas of dead *Molinea* both above and below the water level. In the control site the classifier precisely outlined the various channels and dips in the site, as shown in Fig 19. below.

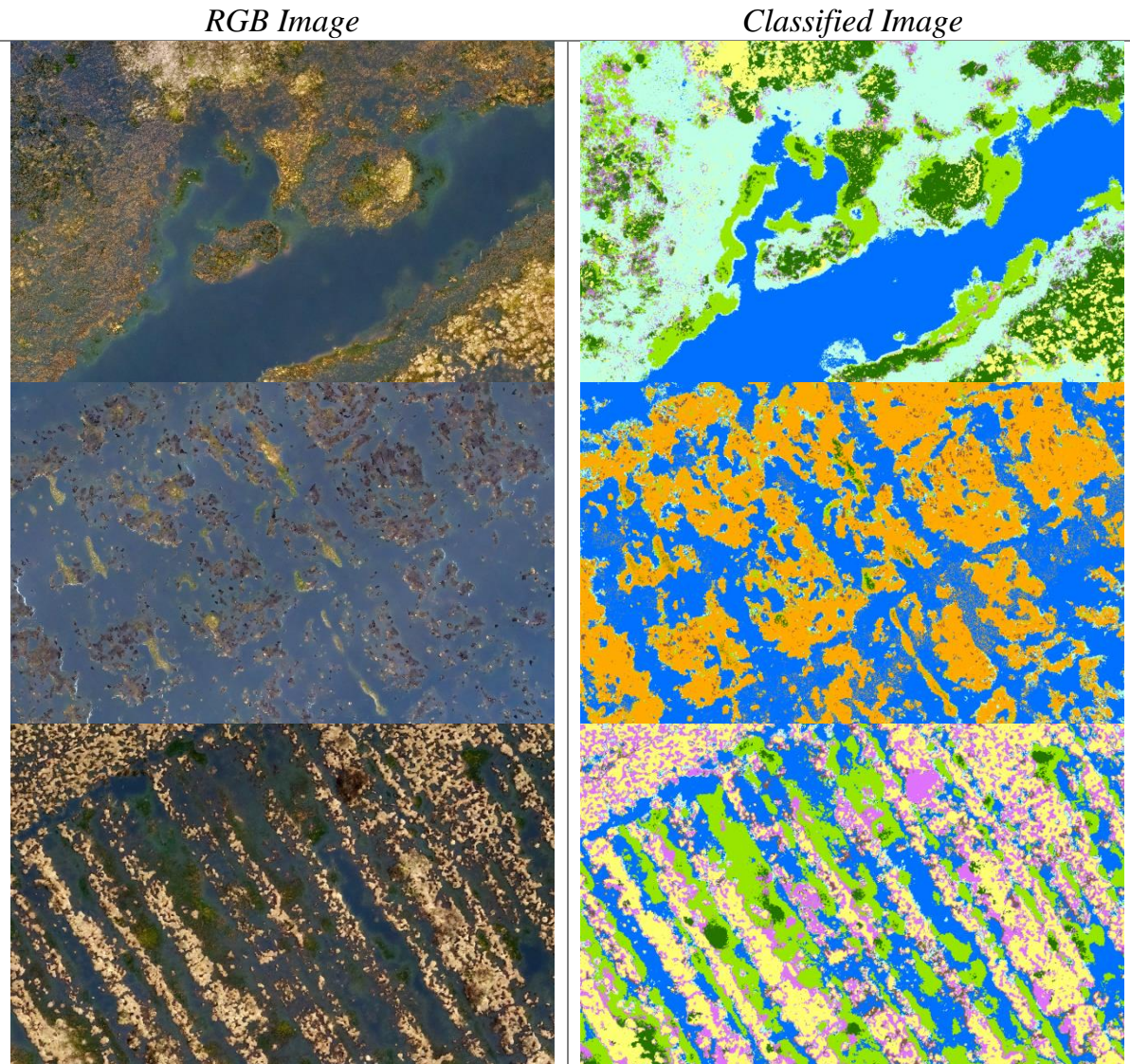


Fig 19. A section in the site inverted in 2000 (top), The site inverted in 2023 (middle), and the control site (bottom), showing the RGB image (left) and the Classified image (right)

In figure 20 below, graph 20 A illustrates the precision, the true positive classifications out of all positive classifications made by the classifier. Precision was consistent across all classes, with peat and open water having the highest precision rates, at 95% and 94% respectively, indicating that these classes were straightforward for the classifier to identify. The other classes showed reasonable high precision between 75-90%, suggesting that the classifier made a few misclassifications overall. *Sphagnum* had the lowest, 75%, showing that the classifier made more misclassifications. Graph 20 B displays the Recall, the positive classification out of all the class instances. Recall was also consistent across each class, with only slight variations. Both open water and bare peat had the highest recall, at 94%, thus confirming that the classifier has few issues correctly identifying this class. Other classes had a recall between 85-90%, demonstrating overall positive classification across all. However,

water/ *Molinea* had the lowest recall, at 84%, indicating that several misclassifications occurred. Graph 20 C presents the F1 score, the agreement between the precision and recall for each class. The score was consistent across the analyses, showing good agreement between precision and recall for the classification with results ranging from 80% to 95%. The highest score was for open water and bare peat, at 95% for both, confirming these classes had the best classification accuracy. The lowest score was recorded for *Sphagnum*, 80%, consistent with its low precision score.

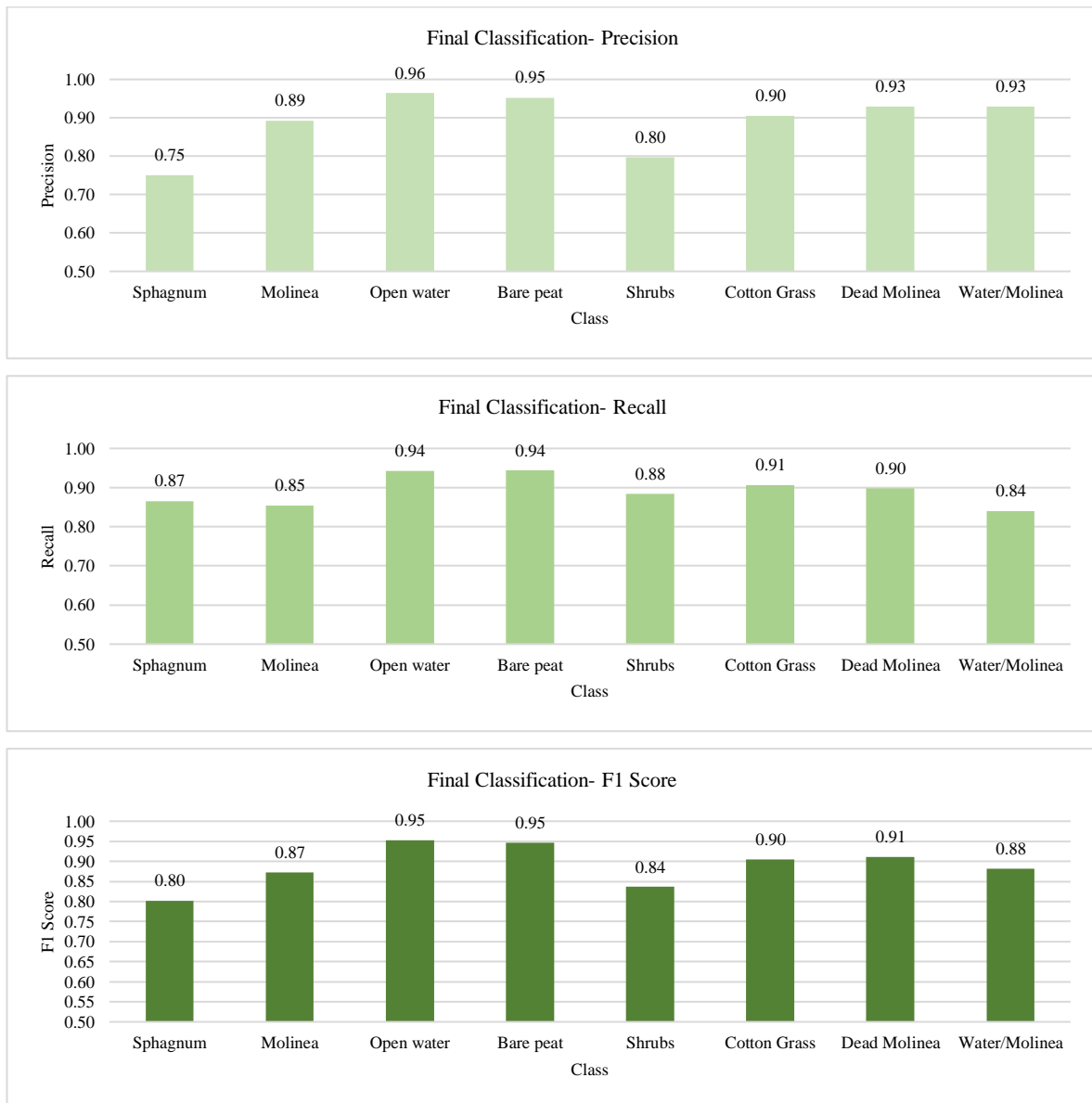


Fig 20. Precision, Recall, and F1 score for the final classification

Class cover

Figure 21 below illustrates the percentage cover of each vegetation class over the three sites.

The 2000 inverted site exhibited the highest cover of water/ *Molinea* with 53%, alongside similar levels of cover of *Sphagnum*, 9%, *Molinea*, 14%, open water, 7%, shrubs, 7%, and cotton grass, 10%. Total *Molinea* cover in this site would be approximately 40% as water/ *Molinea* cover was roughly 50/50. The site contained no bare peat or dead *Molinea*.

The 2023 inverted site was predominantly classified as open water, 43%, with large patches of dead *Molinea*, 38%, and small patches of bare peat, 5%, and *Sphagnum*, 3%. The site showed negligible levels of *Molinea*, shrubs and cotton grass, <1%. The control site had the highest cover of *Molinea*, 32%, shrubs, 22%, and open water, 16%. The site had a similar cover of *Sphagnum*, 10%, and water/ *Molinea*, 9%, alongside low levels of bare peat, 5%, and cotton grass, 5%. Total *Molinea* cover for this site would be roughly 36% when accounting for half the water/ *Molinea* cover. The site inverted in 2000 and the control site both had no Dead *Molinea* cover, consistent with field observations.

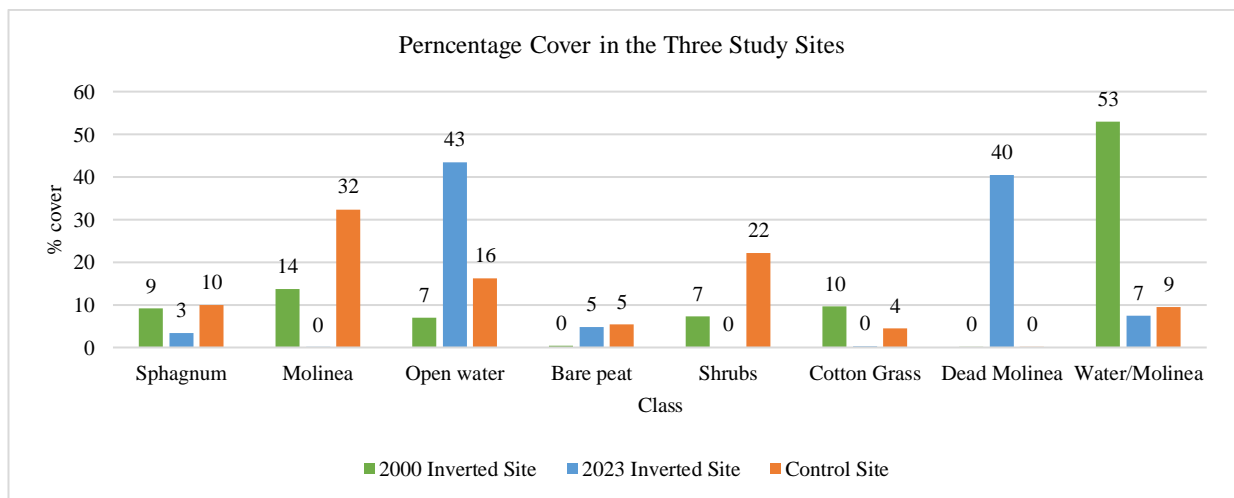


Fig 21. the percent cover of each class in the final classification over each Site.

The inversion work carried out in 2023 would have drastically changed the plant cover since the 2020 vegetation survey so the total cover of just the 2000 inverted and control site was also calculated. Figure 22 below shows the overall coverage of each class over the entire study area. The majority comprises open water, 25%, with large areas of Dead *Molinea*, 17%, water/ *Molinea*, 18%, and *Molinea*, 11%. *Sphagnum* and bare peat each made up 5% of the cover while cotton grass only constituted 3%. When just the 2000 inverted and control sites are examined the cover alters slightly to less open water, 12%,

and more water/ *Molinea*, 26%, Shrubs, 19%, and *Molinea*, 18%. *Sphagnum* increased to 7% and cotton grass to 6%, while bare peat dropped to 4%.

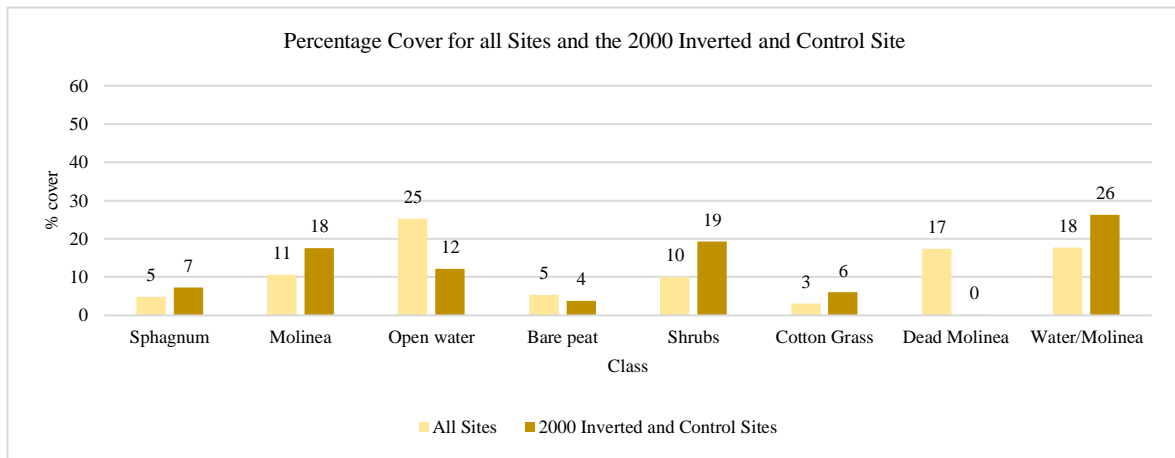


Fig 22. the percentage cover of each class in compartment 14 as a whole, and just in the 2000 inverted site and control site.

Comparison with 2020 vegetation survey

The 2020 survey reported a *Sphagnum* cover of approximately 23%, *Molinea* was approximately 44% when combining three of the sub groups- species poor *Molinea*, gully forms and half of the *Molinea/ Sphagnum* patch cover, and the final significant plant type, cotton grass had 10,2% cover.

	Compartment 14		Compartment 14	
	2014	Surface % of total	2020	Surface % of total
Open water and marsh vegetation			0.04	0.1
peat moss groove vegetation, initial forms	9.01	25.7	7,06	20.1
peat moss groove vegetation, developed forms	0.23	0.7	1,07	3,1
peat moss lump vegetation, well developed	0.35	1.0	0.57	1.6
peat moss lump vegetation, degraded forms			0.15	0.4
communities of Cottongrass, gully forms	3.03	8.6	3.59	10.2
communities of Cottongrass, hummocky forms			0.04	0.1
wet heathland vegetation, species-poor forms			0.14	0.4
wet heathland vegetation, well developed, typical shapes				
wet heathland vegetation, well developed, transitions to raised bog	0.68	1,9	2.58	7.4
pioneer vegetation of wet heathland				
Pipewort vegetation, species-poor forms	3.90	11,1	3.87	11,1
Pipe grass vegetation, gully forms	13.25	37.8	10.15	29.0
Pipe grass vegetation, form with minerotropic peat mosses	0.03	0.1	3,04	8.7
Pipe grass vegetation, forms with raised bog species	1,46	4.2	1,11	3.2
dry heathland vegetation	2.95	8.4	1,36	3.9
crowberry vegetation			0,00	0,0
Winding grass vegetation				
heathland vegetation				
swamp thickets and swamp forests			0.01	0.0
coniferous forests				
Birch-Oak Forests				
Pitrus roughs	0.15	0.4	0.21	0.6
dry roughs	0.05	0.2	0.04	0.1
other				
total	35,09	100.0	35,04	100.0

Fig 23. 2020 vegetation survey by Jongman et al, 202, Translated by Google translate from Dutch to English.

Pipe grass is the colloquial term for Molinea.

4.2. The Multispectral data

The analyses of the NDVI data, as shown in figure 24 below, accurately identified areas of dense and sparse biomass in the study area. Reclassifying each site successfully grouped the pixel values making the different biomass density levels clearer.

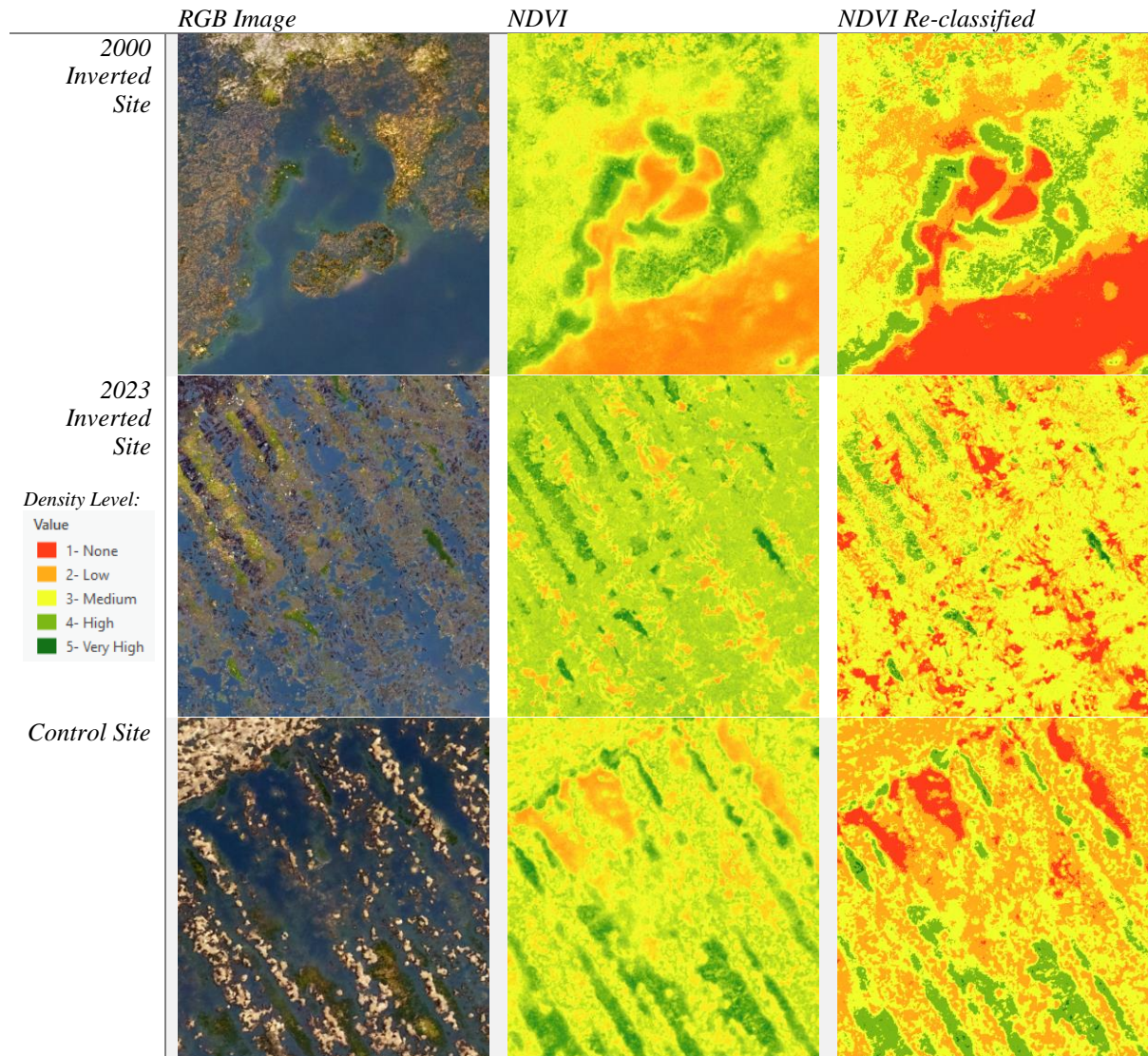


Fig 24. shows the RGB, NDVI, and NDVI reclassified images from each Site. The dark green areas are healthy and have dense vegetation, while the red areas have no vegetation.

The graph in figure 25 below, illustrated the percentage cover of each biomass density level over each site. The 2000 inverted site exhibited the highest biomass density cover, with over 66% of its area having medium to very high density, although less than 0.5% had very high density. The 2023 inverted site had the lowest biomass density cover, with 99% identified as having none to medium density and less than 0.5% having very high density. The control site also reflected low density, with 88% having none to medium density. The 2000 inverted site and the control site displayed similar levels of high density, with the former having 11.1% and the latter 10.7%.

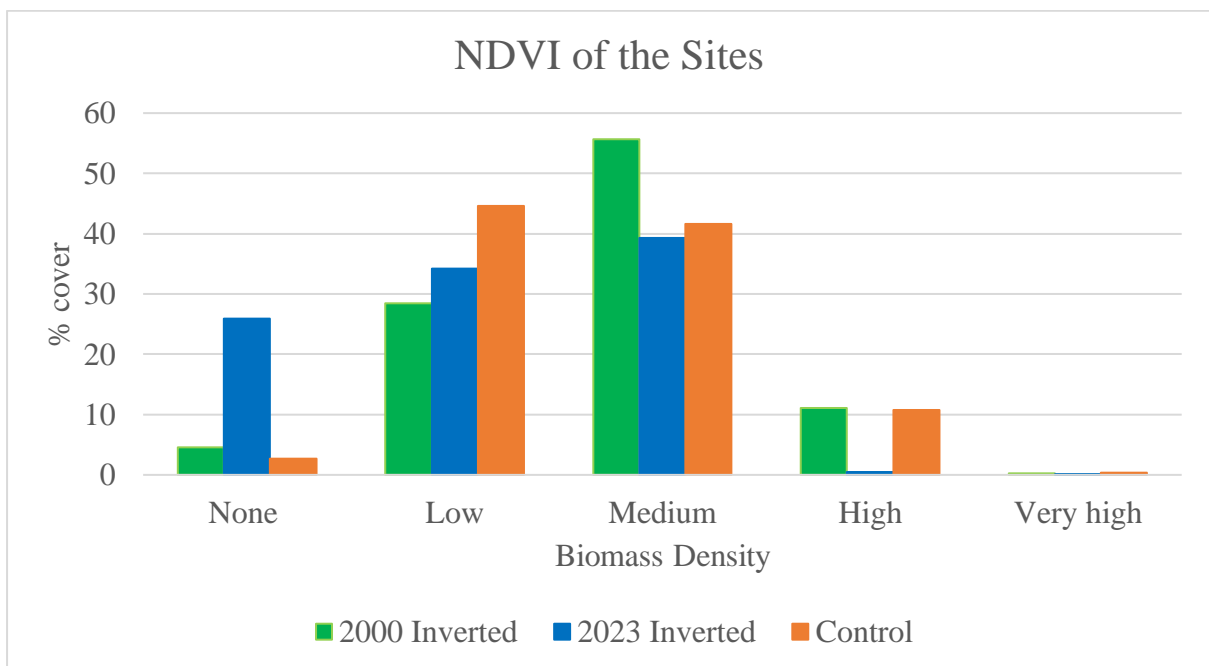


Fig 25. the percentage cover of each biomass density level over the three Sites.

4.3 Comparing Classification and NDVI

In Figure 26 Below some classified areas of each site are compared to the original RGB image and the reclassified NDVI image. Areas classified as having vegetation cover align up exactly with areas identified as having medium to high biomass densities.

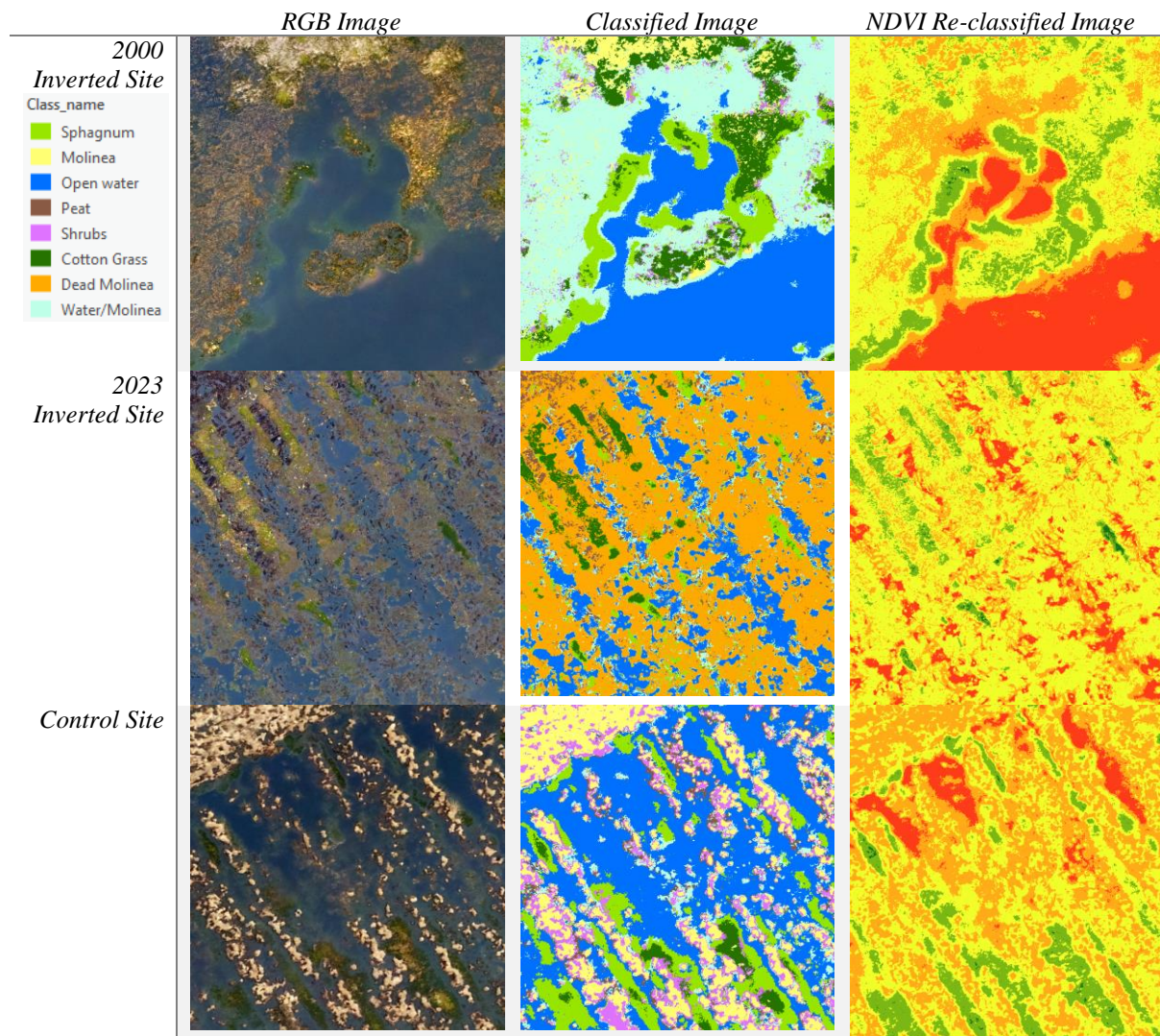


Fig 26. showing the RGB, Classified, and NDVI Re-classified Images for area of each site.

4.4. Hydrological data

Fig 27. shows the historical water level data for compartment 14 before it was split into the three sites in 1999. The original dam was constructed in 1984/85, and the water level was raised to 9.3m above NAP. There was an initial dip in water level following the rewetting but over time the level raised again to 9.4m above NAP in 2000. There were some dips, 1989, and spikes, 1987-88 and 1998, over the time period due to periods of low or high-water level. Overall, the water level stayed consistent over the study period and did not increase dramatically.

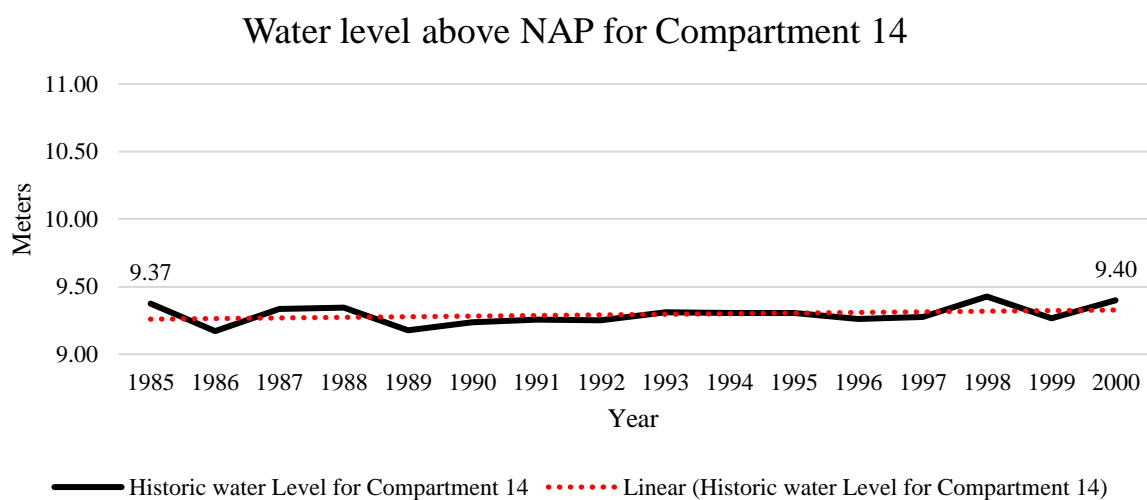


Fig 27. showing the historic water level data from compartment 14 from 1985 to 2000.

Figure 28 below shows the water level from the 2000 inverted site is shown from 2000 to 2022. There was no data available past this period, site management was unsure why. In 2000 the site was split from compartment 14 by the instillation of wooden dams to increase the water level. This was successful as the compartment water level in 1999 was 9.4m NAP and for the site it was 10.5 m NAP after rewetting. The site also underwent the peat inversion restoration method in 2000 which could also have increased the water level. The level has remained consistent over the twenty-two-year period, increasing slightly to 10.8m NAP with a few fluctuations up, 2012, and down 2018, due to periods of increased or decreased rainfall.

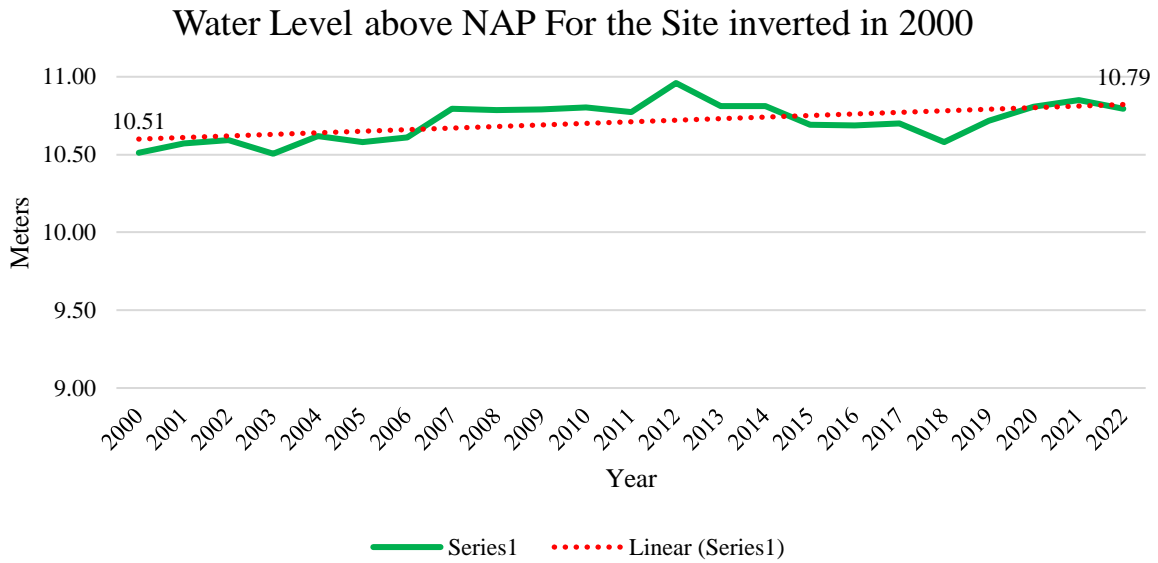


Fig 28. water level for the 2000 inverted site from 2000 to 2022

Figure 29 shows the water level data for the control site from 2000 to 2022. Again, no recent data was available. The site has had a stable water level throughout the recorded period with little variation, from 0.4m NAP at most. The water level has not increased significantly since the instillation of the newer dams in 1999, there were some minor dips, 2018, and spikes, 2010, due to periods of low and high rainfall.

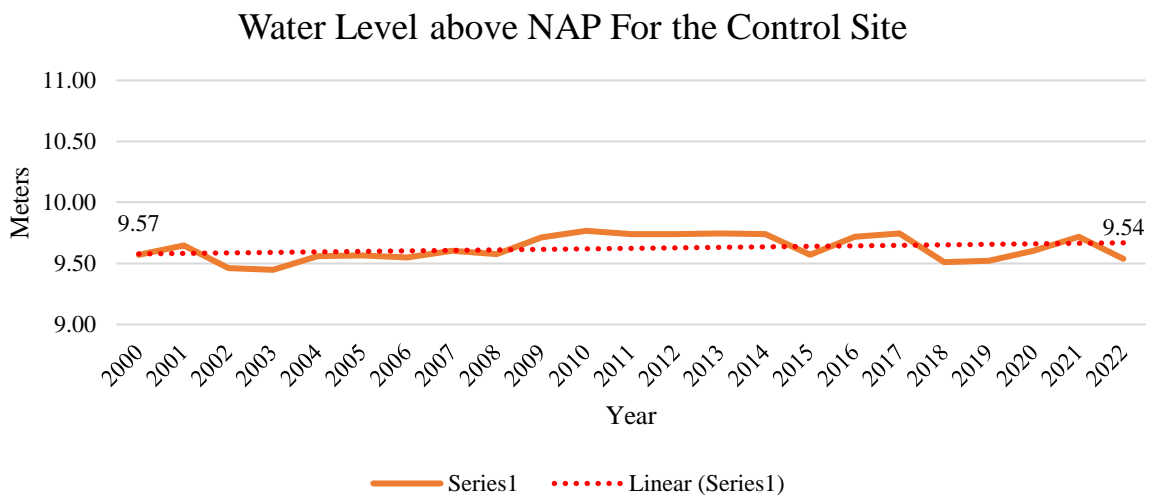


Fig 29. the water level in the control site from 2000 to 2022.

The figure below shows the water level from the site turned in 2023, there was previously no monitoring station in the site and a new one was installed after the inversion took place, so

the period of data is from November 2023 to March 2024. The water level has remained consistent at 10.3/10.4m NAP. It is too soon to tell if the inversion has had a major impact.

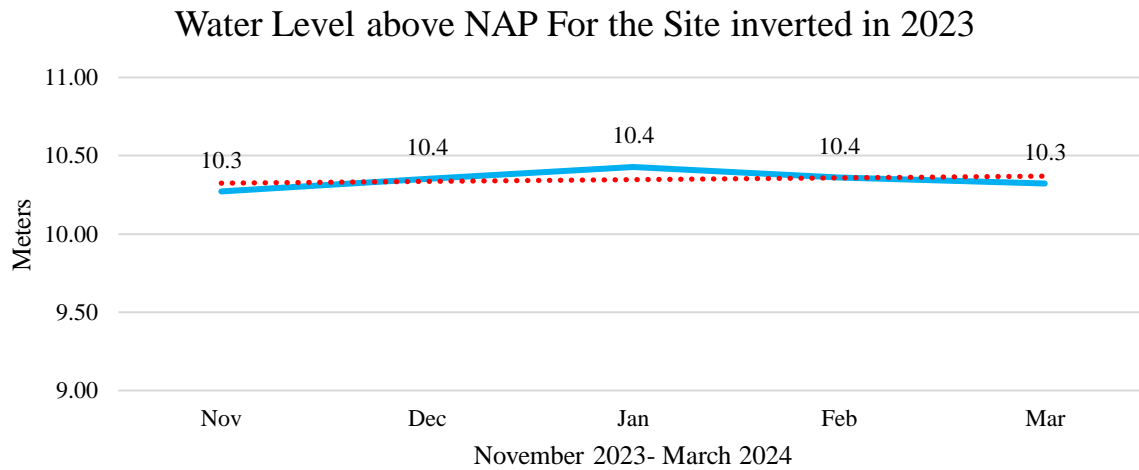


Fig 30. the water level in the control site from November 2023 to March 2024.

5. Discussion

5.1. Random Forest classification

Overall Accuracy of the Classification

The results of the classification were satisfactory; the overall accuracy of 88% achieved by the final classification method is comparable to similar studies which produced accuracy values of 90-95% (Berhane et al., 2018; Beyer et al., 2019; Bhatnagar et al., 2020, 2021; Corcoran et al., 2013). The final classification maps effectively captured much of the fine-scale features and vegetation types in the study area. The incorporation of additional rasters, DEM, and NDVI, which were combined with the RGB image, added significantly more spatial and spectral information for the classifier to work with, improving the accuracy considerably from 71% to 85%. Previous studies that combined raster layers also found this positive effect on accuracy (Amoakoh et al., 2021; Corcoran et al., 2013). The classifier consistently and accurately identified areas of bare peat and water due to their unique spatial and spectral features, making them distinct in the study area (Beyer et al., 2018).

However, it is important to note that these studies focused on healthy raised bog, which had not undergone the level of degradation and restoration work of the study area. As such they contained well-developed microforms and clear topographical features, which aided in the classification (Amoakoh et al., 2021; Corcoran et al., 2013.; Beyer et al, 2018). In contrast, our study area lacked clearly defined microforms due to the past buckwheat cultivation, which disrupted the peat surface (Antala et al., 2022). While the ditches and channels from past drainage in the control site provided topographical differences that aided classification, they did not represent the target microtopography typical of raised bogs. Furthermore, the 2000 inverted site did not have sufficient time to develop microforms, so the use of topographical data for classification was limited. The 2023 inverted site, having undergone inversion so recently, exhibited negligible topographical features, although they did aid in differentiating submerged areas of peat (Figure 16).

The NDVI data also had a noticeable impact on the classification. The higher reflectance of green areas aided in the more accurate identification of *Sphagnum* (Tian et al., 2016; Amoakoh et al, 2021). It was notable in the drone images that algae blooms were not exclusive to the border areas of the 2023 inverted site, as it was with the other two. Instead, it was also observed in areas around floating peat and dead *Molinea* patches. While this could have also been areas of submerged *Sphagnum*, the colour in the images was more in line with the algae seen around the periphery. This caused the classifier to identify these areas as *Sphagnum*. However, when the NDVI raster was included, it did not identify any dense vegetation in these areas, so the classification was corrected to dead *Molinea* and open water. It also corrected the misclassification of water/ *Molinea* in the 2000 inverted site, some areas of which have been identified as dead *Molinea*. As such, the addition of the NDVI raster highlighted the difference in reflectance between the two classes and corrected the misclassification (Tian et al., 2016; Amoakoh et al., 2021).

The timing of the survey most likely influenced classification accuracy. In March, *Molinea* patches are a distinctive yellow colour during the transition from Winter to Spring. This differentiated it clearly from the other classes. In comparison the cotton grass was flowering for spring and had dark green foliage, which caused some confusion between it and *Sphagnum*, the yellow flowers present at the time aided in identifying samples but maybe were not spectrally different enough for the classifier. Areas of shrub vegetation appeared dark brown at the time of the survey, leading to misclassifications of areas of bare peat as shrub. This was a particular issue in the control site where small dips and holes in the site,

which contained peat, shaded water or *Sphagnum*, were identified as shrubs, as seen in Figure 16 in the results.

Sphagnum and cotton grass were particularly similar in the RGB images, which caused the classifier to misclassify them on several occasions. This issue was less pronounced in the control site, where the elevation data from the DEM likely aided the classifier in differentiating the two as cotton grass predominantly occupied the higher ground while *Sphagnum* populated the ditches and gullies caused by the previous agrarian land use (Amoakoh et al., 2021; Corcoran et al., 2013.; Beyer et al, 2018). In the 2000 inverted plot, the elevation data was not as informative for the classifier as typical bog microforms have not yet developed so there were more misclassifications between *Sphagnum* and cotton grass there.

Comparing the Class Cover Between Sites

Both the 2000 inverted site and the control had similar *Sphagnum* and *Molinea* cover. This was surprising as it was expected that the 2000 inverted site would contain more *Sphagnum* and less *Molinea* than the control, due to the peat inversion and higher water level in the former site. This unexpected result could be due to misclassification as the classifier struggled to accurately classify *Sphagnum* and particularly submerged areas of *Sphagnum*, which could have been distorted in the images due to water. Much of the *Sphagnum* in the control site was observed in the ditches and gullies, these areas were often overshadowed by *Molinea* and shrubs (Altenburg et al., 1993; Tomassen et al., 2010), causing them to appear darker on the images and to subsequently be misclassified (Buchsteiner et al., 2023).

The *Molinea* cover in the 2000 inverted site was predominately from the water/*Molinea* class for which the proportion of *Molinea* to water was estimated, some areas contained more or less *Molinea*. This could have been overestimated, impacting the results. Much of the control site was classified as *Molinea* with even small patches being precisely identified from surrounding water or vegetation. This is in line with what was observed during fieldwork, where the site looked to be entirely covered in *Molinea* with some areas of shrubs, patches of sphagnum could only be seen in ditches or areas with more open water. As previously mentioned, this caused difficulties in accurately identifying the full sphagnum cover.

The 2023 inverted site, having undergone recent inversion, showed minimal vegetation cover. It was positive to see some *Sphagnum* cover on the site, and with the high-water table and absence of live *Molinea*, conditions look optimal for its expansion in the coming decades (Huth et al., 2022).

Comparison to the 2020 Vegetation Survey

Comparing this classification result to the 2020 vegetation survey provided valuable insights into the classification's success. The cover of all plant types had decreased, most likely due to the inversion of the site in 2023, which drowned its vegetation cover. Even when this site was excluded and just the 2000 inverted site and control site were utilised, the cover of the target species, *Sphagnum*, was significantly less than was recorded in the 2020 survey. This is unexpected as conditions have not been so adverse in the area that cover would reduce to this degree. The reduction is likely due to misclassification as *Sphagnum* did have the lowest F1 score of all the classes. This was probably caused by many patches being partially submerged underwater in the 2000 inverted site, which can confuse the classifier, especially in water-land boundary areas (Tian et al., 2016; Buchsteiner et al., 2023). *Sphagnum* also populated many ditches in the control site which were often overshadowed by *Molinea* (Altenburg et al., 1993; Tomassen et al., 2010), causing misclassification issues as discussed earlier. These conditions were observed during fieldwork. Cotton grass coverage also appeared to have decreased but this is most likely due to the 2023 inversion work. *Molinea* cover had not changed much, the 2020 survey reported a similar cover as was classified in this study. This was unexpected as the inversion work was implemented to reduce *Molinea* coverage. Misclassifications could be to blame or the estimations of coverage, as the water/ *Molinea* class varied in its *Molinea* density so future surveys should more accurately estimate the proportions. However, the inverted sight is still in the early stages of development so while lack of clear reductions in *Molinea* may not be visible yet, future surveys may yield more positive results.

Overall, few conclusions can be drawn from the 2023 inverted sight. The work was carried out so recently that the site has not had time for vegetation to regrow or the target species, *Sphagnum*, to re-establish or expand. Based on the *Sphagnum* cover of the site inverted two decades ago there are positive signs that cover can re-establish quickly. The 2023 site is more than double the size of the 2000 site so future surveys comparing the recovery of the two will be insightful.

5.2. Analyses of the Multispectral Data

The 2000 inverted site had the highest cover of high-density biomass indicating the widespread coverage of vegetation present. This outcome was anticipated, as dense green

areas of vegetation were observed on the site during fieldwork. At the time of the survey the *Molinea* in the site was a distinctive yellow colour, which likely resulted in lower reflectance than denser green areas (Tian et al., 2016; Amoakoh et al, 2021). This would have caused its density to be underestimated, but did allow for a focus on *Sphagnum* and cotton grass coverage which were both bright green at the time of the survey and so would have reflected well. The control site was noted to have high *Molinea*, and shrub cover during field work, which was yellow and brown at the time and so would have a lower reflectance (Tian et al., 2016; Amoakoh et al, 2021). Therefore, the NDVI scores for both were under classified on the site. While in the 2000 inverted site this aided in identifying dense green areas of *Sphagnum* and cotton grass, the control site had such extensive *Molinea* and Shrub, that *Sphagnum* patches were overshadowed and so not picked up by the NDVI calculation. The 2023 inverted site showed the lowest cover of dense biomass, as anticipated, due to the recent restoration work that submerged all existing vegetation, thus there would be minimal reflectance.

5.3. Hydrological data

The hydrological data showed little increase since the instillation of the original dams in 1984/85, staying stable with only minor fluctuations until 1999 when the new dams were installed and the compartment divided into the three sites. This caused a significant increase in the water level of the 2000 inverted sight. This successful rewetting would have aided in the reestablishment and expansion of typical bog plant species, particularly target species like *Sphagnum* (Crowley et al., 2021; Günther et al., 2020). The 2023 inverted site also showed a heightened water level compared to the historical data, although since this measurement station was installed after the peat inversion work it doesn't give details on the water level post 1999 dam instillation. The current high-water level is a positive sign that should lead to the quick recovery and expansion of typical bog plant species in the site (Renou-Wilson et al., 2019; Huth et al., 2022) and prevent *Molinea* from dominating once again. The control site had the lowest water level of the three which could explain why there was still much *Molinea* coverage despite the installation of new dams to maintain a high-water level. Increased water levels should encourage typical bog plant species to grow while creating adverse conditions for domineering species like *Molinea* (Huth et al., 2022), but the water level in the control site has only increase marginally since the addition of new dams in 1999. The areas uneven topography, from the buckwheat cultivation, could be exacerbating the issue as rainwater drains quickly into the ditches and isn't retained in elevated areas to

encourage *Sphagnum* growth (Clymo, 1973). *Molinea* possess deep roots which can tap into water deep in the ground, thus it can thrive even when water levels are low (Altenburg et al., 1993; Tomassen et al., 2010).. That paired with its extensive cover in the control site mean a new approach may be necessary to speed up restoration and achieve the goals of Natuurmonumenten (Altenburg et al., 2017).

5.4.Future research

To improve future classification of the study area it is recommended to ensure all equipment is in working order. During processing of the drone images, it was noticed that the calibration plate had been marginally off due to a sticker on the back that could not be seen in person but showed through on the calibration images. This could have thrown off the calibration of the final drone images when adjusting them for the reflectance and light at the time of the survey.

The final sample set for this survey was taken from certain areas around the periphery of the study sites that were accessible by foot, this constrained the training and sample data as a randomised sample set would more accurately represent the proportion of each class. The number of samples was increased to account for this and ensure accurate results, but future classification could try a more randomised set to reduce possible bias.

Due to the time-consuming nature of collecting samples manually in field the original ground truthing data contained five to twenty-six samples per class, which is a significant difference. Therefore, all the samples used for the training data set were manually identified on the drone images, efforts were made to take samples from a variety of examples of each class and to ensure each was correct but human bias could have been introduced. Future analyses should ensure enough time for sample collection or plan extra field days.

Undertaking the survey in March aided the classification as classes were more distinguishable, *Molinea* was a distinctive yellow colour. However other classes like cotton grass were quite spectrally similar to *Sphagnum*, which resulted in some misclassification. Future studies should gather and layer data from across the year to provide more information to the classifier.

6. Conclusion

In conclusion, this study aimed to investigate how the peat inversion restoration technique has impacted the cover of target species in the Fochteloërveen, particularly *Sphagnum* and *Molinea*. A drone survey and the Random Forest classification were used to classify the plant types of present, this yielded accurate classification maps of the area which could differentiate between the homogenous fine details of the peatland vegetation cover. When the class cover was analysed, it revealed that the 2000 inverted site had similar levels of *Sphagnum* and *Molinea* cover compared to the control site, which was unexpected given the anticipated improvements from the peat inversion and higher water levels in the former. This result was likely due to misclassification issues, particularly with submerged *Sphagnum* areas, which were distorted in the imagery by water.

The 2023 inverted site showed little vegetation recovery as it had recently undergone inversion, yet the presence of some *Sphagnum* cover and the absence of live *Molinea* indicate promising conditions for future expansion. Comparing the classification results with the 2020 vegetation survey highlighted a decrease in *Sphagnum* cover across the study area, suggesting that the inversion work has temporarily impacted the overall plant cover of the study area.

While the study gives valuable insights into the current state of bog restoration efforts, it also underscores the need for further monitoring and research. The application of modern drone surveying and the Random Forest classification method allows for the efficient analyses and creation of comparable vegetation maps of the sites. Continued refinement and study will only improve these results. As the 2023 inverted site has not yet had sufficient time for vegetation to regrow or for *Sphagnum* to re-establish and expand, future surveys will be crucial in assessing the long-term effectiveness of restoration strategies. Overall, this research emphasizes the necessity of adaptive management in peatland restoration and the potential for rapid recovery of *Sphagnum* when optimal conditions are established.

7. References

- Altenburg, W., Bijkerk, W., Douwes, R., & Straathof, N. (2017). Neergang en opkomst van het Fochteloërveen: Resultaten van 30 jaar hoogveenherstel. *De Levende Natuur*, 118(3), 79–84.
- Altenburg, W., Jansen, H., & van der Veen, W. S. (1993). *VEGETATIE-ONTWIKKELING IN HET FOCHTELOERVEEN VAN DE JAREN '60 TOT 1992*. A&W-rapport 52 Veenwouden.
- Altenburg, W., & van der Veen, K. (2003). *VEGETATIE-ONTWIKKELING IN HET FOCHTELOERVEEN VAN DE PERIODE 1992—2002*. A&W-rapport 52 Veenwouden.
- Amoakoh, A. O., Aplin, P., Awuah, K. T., Delgado-Fernandez, I., Moses, C., Alonso, C. P., Kankam, S., & Mensah, J. C. (2021). Testing the Contribution of Multi-Source Remote Sensing Features for Random Forest Classification of the Greater Amanzule Tropical Peatland. *Sensors*, 21(10), Article 10. <https://doi.org/10.3390/s21103399>
- An, S., & Verhoeven, J. T. A. (2019). Wetland Functions and Ecosystem Services: Implications for Wetland Restoration and Wise Use. *Wetlands: Ecosystem Services, Restoration and Wise Use*, 238. https://doi.org/10.1007/978-3-030-14861-4_1
- Andersen, R., Farrell, C., Graf, M., Muller, F., Calvar, E., Frankard, P., Caporn, S., & Anderson, P. (2017). An overview of the progress and challenges of peatland restoration in Western Europe. *Restoration Ecology*, 25(2), 271–282. <https://doi.org/10.1111/rec.12415>
- Andersen, R., Poulin, M., Borcard, D., Laiho, R., Laine, J., Vasander, H., & Tuittila, E.-T. (2011). Environmental control and spatial structures in peatland vegetation. *Journal of Vegetation Science*, 22(5), 878–890. <https://doi.org/10.1111/j.1654-1103.2011.01295.x>

- Antala, M., Juszczak, R., van der Tol, C., & Rastogi, A. (2022). Impact of climate change-induced alterations in peatland vegetation phenology and composition on carbon balance. *Science of The Total Environment*, 827, 154294.
<https://doi.org/10.1016/j.scitotenv.2022.154294>
- Badda, H., Cherif, E. K., Boulaassal, H., Wahbi, M., Yazidi Alaoui, O., Maatouk, M., Bernardino, A., Coren, F., & El Kharki, O. (2023). Improving the Accuracy of Random Forest Classifier for Identifying Burned Areas in the Tangier-Tetouan-Al Hoceima Region Using Google Earth Engine. *Remote Sensing*, 15(17), Article 17.
<https://doi.org/10.3390/rs15174226>
- Barbosa, B. D. S., Ferraz, G. A. S., Goncalves, L. M., Marin, D. B., Maciel, D. T., Ferraz, P. F. P., & Rossi, G. (2019). RGB vegetation indices applied to grass monitoring: A qualitative analysis. *Agronomy Research*, 17. <https://doi.org/10.15159/AR.19.119>
- Berhane, T. M., Lane, C. R., Wu, Q., Autrey, B. C., Anenkhonov, O. A., Chepinoga, V. V., & Liu, H. (2018). Decision-Tree, Rule-Based, and Random Forest Classification of High-Resolution Multispectral Imagery for Wetland Mapping and Inventory. *Remote Sensing*, 10(4), Article 4. <https://doi.org/10.3390/rs10040580>
- Beyer, F., Jurasinski, G., Couwenberg, J., & Grenzdörffer, G. (2019). Multisensor data to derive peatland vegetation communities using a fixed wing unmanned aerial vehicle. *International Journal of Remote Sensing*, 40(24), 9103–9125.
<https://doi.org/10.1080/01431161.2019.1580825>
- Bhatnagar, S., Gill, L., & Ghosh, B. (2020). Drone Image Segmentation Using Machine and Deep Learning for Mapping Raised Bog Vegetation Communities. *Remote Sensing*, 12(16). <https://doi.org/10.3390/rs12162602>
- Bhatnagar, S., Gill, L., Regan, S., Waldren, S., & Ghosh, B. (2021). A nested drone-satellite approach to monitoring the ecological conditions of wetlands. *ISPRS Journal of*

Photogrammetry and Remote Sensing, 174, 151–165.

<https://doi.org/10.1016/j.isprsjprs.2021.01.012>

Brouns, K., Keuskamp, J. A., Potkamp, G., Verhoeven, J. T. A., & Hefting, M. M. (2016).

Peat origin and land use effects on microbial activity, respiration dynamics and exoenzyme activities in drained peat soils in the Netherlands. *Soil Biology and*

Biochemistry, 95, 144–155. <https://doi.org/10.1016/j.soilbio.2015.11.018>

Buchsteiner, C., Baur, P., & Glatzel, S. (2023). Spatial Analysis of Intra-Annual Reed

Ecosystem Dynamics at Lake Neusiedl Using RGB Drone Imagery and Deep

Learning. *Remote Sensing*, 15, 3961. <https://doi.org/10.3390/rs15163961>

Buznego, C. (2023). *Design and evaluation of a method to monitor vegetation development in*

Marker Wadden using RGB and multi-spectral drone imagery. Utrecht University.

Casparie, W. A. (1993). The Bourtanger Moor: Endurance and vulnerability of a raised bog

system. *Hydrobiologia*, 265. <https://doi.org/10.1007/BF00007269>

Corcoran, J. M., Knight, J. F., & Gallant, A. L. (2013). Influence of Multi-Source and Multi-

Temporal Remotely Sensed and Ancillary Data on the Accuracy of Random Forest

Classification of Wetlands in Northern Minnesota. *Remote Sensing*, 5(7), Article 7.

<https://doi.org/10.3390/rs5073212>

Couwenberg, J., & Joosten, H. (1999). Pools as missing links: The role of nothing in the

being of mires. Patterned mires and mire pools—origin and development, 87-102.

Patterned Mires and Mire Pools—Origin and Development, 87–102.

Crowley, W., Smith, G. F., Mackin, F., Regan, S., Fernandez Valverde, F., & Eakin, M.

(2021). Recovery of the vegetation of a cutover raised bog in Ireland following

rewetting measures. *Biology and Environment: Proceedings of the Royal Irish*

Academy, 121(2). <https://doi.org/10.1353/bae.2021.0011>

- De Bruin, J., Barel, J. M., & Temmink, R. (2023). *Raised peat restoration in the Fochteloërveen: An integrated approach with nature-based solutions*. Natuurmonumenten.
- Diaz-Delgado, R., Cazacu, C., & Adamescu, M. (2018). Rapid Assessment of Ecological Integrity for LTER Wetland Sites by Using UAV Multispectral Mapping. *Drones*, 3(1). <https://doi.org/10.3390/drones3010003>
- Dise, N. B. (2009). Peatland Response to Global Change. *Science*, 326(5954), 810–811. <https://doi.org/10.1126/science.1174268>
- Dronova, I. (2015). Object-Based Image Analysis in Wetland Research: A Review. *Remote Sensing*, 7(5), Article 5. <https://doi.org/10.3390/rs70506380>
- ERSI. (2024). *Raster—ArcGIS Pro / Documentation*. ArcGIS Pro Help. <https://pro.arcgis.com/en/pro-app/latest/arcpy/classes/raster-object.htm>
- Fluet-Chouinard, E., Stocker, B. D., Zhang, Z., Malhotra, A., Melton, J. R., Poulter, B., Kaplan, J. O., Goldewijk, K. K., Siebert, S., Minayeva, T., Hugelius, G., Joosten, H., Barthelmes, A., Prigent, C., Aires, F., Hoyt, A. M., Davidson, N., Finlayson, C. M., Lehner, B., ... McIntyre, P. B. (2023). Extensive global wetland loss over the past three centuries. *Nature*, 614(7947), 281–286. <https://doi.org/10.1038/s41586-022-05572-6>
- Green, A. J., Alcorlo, P., Peeters, E. T., Morris, E. P., Espinar, J. L., Bravo-Utrera, M. A., Bustamante, J., Diaz-Delgado, R., Koelmans, A. A., Mateo, R., Mooij, W. M., Rodriguez-Rodriguez, M., van Nes, E. H., & Scheffer, M. (2017). Creating a safe operating space for wetlands in a changing climate. *Frontiers in Ecology and the Environment*, 15(2). <https://doi.org/10.1002/fee.1459>
- Günther, A., Barthelmes, A., Huth, V., Joosten, H., Jurasinski, G., Koebisch, F., & Couwenberg, J. (2020). Prompt rewetting of drained peatlands reduces climate

- warming despite methane emissions. *Nature Communications*, 11.
<https://doi.org/10.1038/s41467-020-15499-z>
- Guo, M., Li, J., Sheng, C., Xu, J., & Wu, L. (2017). A Review of Wetland Remote Sensing. *Sensors*, 17(4). <https://doi.org/10.3390/s17040777>
- Hu, S., Niu, Z., Chen, Y., Li, L., & Zhang, H. (2017). Global wetlands: Potential distribution, wetland loss, and status. *Science of The Total Environment*, 586, 319–327.
<https://doi.org/10.1016/j.scitotenv.2017.02.001>
- Huth, V., Günther, A., Bartel, A., Gutekunst, C., Heinze, S., Hofer, B., Jacobs, O., Koebisch, F., Rosinski, E., Tonn, C., Ullrich, K., & Jurasinski, G. (2022). The climate benefits of topsoil removal and introduction in raised bog restoration. *Restoration Ecology*, 30(1), e13490. <https://doi.org/10.1111/rec.13490>
- Jeziorska, J. (2019). UAS for Wetland Mapping and Hydrological Modeling. *Remote Sensing*, 11(17). <https://doi.org/10.3390/rs11171997>
- Jongman, M. (2021). *VEGETATIEKARTERING & FLORAKARTERING FOCHTELOËRVEEN EN NORGERHOLT 2020*. EGG-Consultant.
- Joosten, H. (1993). DENKEN WIE EIN HOCHMOOR: Hydrologische Selbstregulation von Hochmooren und deren Bedeutung für Wiedervernässung und Restauration. *TELMA - Berichte der Deutschen Gesellschaft für Moor- und Torfkunde*, 23, 95–115.
<https://doi.org/10.23689/fidgeo-5882>
- Jurasinski, G., Ahmad, S., Anadon-Rosell, A., Berendt, J., Beyer, F., Bill, R., Blume-Werry, G., Couwenberg, J., Günther, A., Joosten, H., Koebisch, F., Köhn, D., Koldrack, N., Kreyling, J., Leinweber, P., Lennartz, B., Liu, H., Michaelis, D., Mrotzek, A., ... Wrage-Mönnig, N. (2020). From Understanding to Sustainable Use of Peatlands: The WETSCAPES Approach. *Soil Systems*, 4(1), Article 1.
<https://doi.org/10.3390/soilsystems4010014>

- Lamers, L. P. M., Bobbink, R., & Roelofs, J. G. M. (2000). Natural nitrogen filter fails in polluted raised bogs. *Global Change Biology*, 6(5), 583–586.
<https://doi.org/10.1046/j.1365-2486.2000.00342.x>
- Loisel, J., & Gallego-Sala, A. (2022). Ecological resilience of restored peatlands to climate change. *Communications Earth & Environment*, 208.
<https://www.nature.com/articles/s43247-022-00547-x>
- Mathema, A. B. (2005). *Monitoring of peat bog restoration* [This study will expand the understanding of wetland restoration techniques and the application of UAS in evaluating them. Better identification and vegetation mapping can reveal how a peatland is developing after a restoration allowing more effective restoration work that can restore these areas back to their natural dynamics or close to the. The use of UAS in this area is cheaper, faster and more accurate than other methods giving up to date information to better plan for future projects.].
https://library.itc.utwente.nl/papers_2005/msc/nrm/mathema.pdf
- Millard, K., & Richardson, M. (2015). On the Importance of Training Data Sample Selection in Random Forest Image Classification: A Case Study in Peatland Ecosystem Mapping. *Remote Sensing*, 7(7), Article 7. <https://doi.org/10.3390/rs70708489>
- Müller, J., & Joos, F. (2021). Committed and projected future changes in global peatlands – continued transient model simulations since the Last Glacial Maximum. *Biogeosciences*, 18. <https://doi.org/10.5194/bg-18-3657-2021>
- Oosterwerld, E., & van den Brink, H. (2010). *Natuurvisie 2009-2029: Fochteloërveen / Hydrotheek* (No. 1936764). Natuurmonumenten, Regio Groningen, Friesland en Drenthe. <https://library.wur.nl/WebQuery/hydrotheek/1936764>
- Qiu, C., Zhu, D., Ciais, P., Guenet, B., & Peng, S. (2020). The role of northern peatlands in the global carbon cycle for the 21st century. *Global Ecology and Biogeography*, 29(5), 956–973. <https://doi.org/10.1111/geb.13081>

- Quik, C., Van der Velde, Y., Candel, J. H. J., Steinbuch, L., van Beek, R., & Wallinga, J. (2023). Faded landscape: Unravelling peat initiation and lateral expansion at one of northwest Europe's largest bog remnants. *Biogeosciences*, *20*(3), 695–718. <https://doi.org/10.5194/bg-20-695-2023>
- Rasanen, A., Aurela, M., Juutinen, S., Kumpula, T., Lohila, A., Penttila, T., & Virtanen, T. (2019). Detecting northern peatland vegetation patterns at ultra-high spatial resolution. *Remote Sensing in Ecology and Conservation*, *6*(4). <https://doi.org/10.1002/rse2.140>
- Rasanen, A., Juutinen, S., Kalacska, M., Aurela, M., Heikkinen, P., Maenpaa, K., Rimali, A., & Virtanen, T. (2020). Peatland leaf-area index and biomass estimation with ultra-high resolution remote sensing. *GIScience & Remote Sensing*, *57*. <https://doi.org/10.1080/15481603.2020.1829377>
- Räsänen, A., Juutinen, S., Tuittila, E.-S., Aurela, M., & Virtanen, T. (2019). Comparing ultra-high spatial resolution remote-sensing methods in mapping peatland vegetation. *Journal of Vegetation Science*, *30*(5). <https://doi.org/10.1111/jvs.12769>
- Regan, S., Flynn, R., Gill, L., Naughton, O., & Johnston, P. (2019). Impacts of groundwater drainage on peatland subsidence and its ecological implications on an Atlantic raised bog. *Water Resources Research*, *55*. <https://doi.org/10.1029/2019WR024937>
- Renou-Wilson, F., Moser, G., Fallon, D., Farrell, C. A., Muller, C., & Wilson, D. (2019). Rewetting degraded peatlands for climate and biodiversity benefits: Results from two raised bogs. *Ecological Engineering*, *127*. <https://doi.org/10.1016/j.ecoleng.2018.02.014>
- Robroek, B. J. M., Jassey, V. E. J., Payne, R. J., Marti, M., Bragazza, L., Bleeker, A., Buttler, A., Caporn, S. J. M., Dise, N. B., Kattge, J., Zając, K., Svensson, B. H., van Ruijven, J., & Verhoeven, J. T. A. (2017). Taxonomic and functional turnover are decoupled in

- European peat bogs. *Nature Communications*, 8. <https://doi.org/10.1038/s41467-017-01350-5>
- Robroek, B. J. M., van Ruijven, J., Schouten, M. G. C., Breeuwer, A., Crushell, P. H., Berendse, F., & Limpens, J. (2009). Sphagnum re-introduction in degraded peatlands: The effects of aggregation, species identity and water table. *Basic and Applied Ecology*, 10(8), 697–706. <https://doi.org/10.1016/j.baae.2009.04.005>
- Sahar, N., Robroek, B. J. M., Mills, R. T. E., Dumont, M. G., & Barel, J. M. (2022). Peatland Plant Functional Type Effects on Early Decomposition Indicators are non-pervasive, but Microhabitat Dependent. *Wetlands*, 98. <https://doi.org/10.1007/s13157-022-01626-7>
- Salimi, S., Almuktar, S. A. A. A. N., & Scholz, M. (2021). Impact of climate change on wetland ecosystems: A critical review of experimental wetlands. *Journal of Environmental Management*, 286. <https://doi.org/10.1016/j.jenvman.2021.112160>
- Scholz, M., & Salimi, S. (2021). Impact of future climate scenarios on peatland and constructed wetland water quality: A mesocosm experiment within climate chambers. *Journal of Environmental Management*, 289. <https://doi.org/10.1016/j.jenvman.2021.112459>
- Schouwenaars, J. M., & Gosen, A. M. (2007). The sensitivity of Sphagnum to surface layer conditions in a re-wetted bog: A simulation study of water stress. *Mires and Peat*, 2. <https://edepot.wur.nl/37014>
- Shepard, H. E. R., Temmink, R., Martin, I., Marin, A., Cruisjen, P. M. J. M., & Robroek, B. J. M. (2023). Post-fire peatland recovery by peat moss inoculation depends on water table depth. *Journal of Applied Ecology*, 60, 673–684. <https://doi.org/10.1111/1365-2664.14360>
- Shi, X., Thornton, P. E., Ricciuto, D. M., Hanson, P. J., Mao, J., Sebestyen, S., Griffiths, N., & Bisht, G. (2015). Representing northern peatland microtopography and hydrology

- within the Community Land Model. *Biogeosciences*, 12. <http://dx.doi.org/10.5194/bg-12-6463-2015>
- Simpson, G., Nichol, C., Wade, T., Helfter, C., Hamilton, A., & Gibson-Poole, S. (2024). Species-Level Classification of Peatland Vegetation Using Ultra-High-Resolution UAV Imagery. *Drones*, 8, 97. <https://doi.org/10.3390/drones8030097>
- Smolders, A. J. P., Tomassen, H. B. M., Lamers, L. P. M., Lomans, B. P., & Roelofs, J. G. M. (2002). Peat bog restoration by floating raft formation: The effects of groundwater and peat quality. *Journal of Applied Ecology*, 39(3), 391–401. <https://doi.org/10.1046/j.1365-2664.2002.00724.x>
- Smolders, A. J. P., Tomassen, H. B. M., van Mullekom, M., Lamers, L. P. M., & Roelofs, J. G. M. (2003). Mechanisms involved in the re-establishment of Sphagnum-dominated vegetation in rewetted bog remnants. *Wetlands Ecology and Management*, 11(6), 403–418. <https://doi.org/10.1023/B:WETL.0000007195.25180.94>
- Steenvoorden, J., Bartholomeus, H., & Limpens, J. (2023). Less is more: Optimizing vegetation mapping in peatlands using unmanned aerial vehicles (UAVs). *International Journal of Applied Earth Observation and Geoinformation*, 117. <https://doi.org/10.1016/j.jag.2023.103220>
- Steenvoorden, J., & Limpens, J. (2023a). Upscaling peatland mapping with drone-derived imagery: Impact of spatial resolution and vegetation characteristics. *GIScience & Remote Sensing*, 60. <https://doi.org/10.1080/15481603.2023.2267851>
- Steenvoorden, J., & Limpens, J. (2023b). Upscaling peatland mapping with drone-derived imagery: Impact of spatial resolution and vegetation characteristics. *GIScience & Remote Sensing*, 60(1), 2267851. <https://doi.org/10.1080/15481603.2023.2267851>
- Steenvoorden, J., Limpens, J., Crowley, W., & Schouten, M. G. C. (2022). There and back again: Forty years of change in vegetation patterns in Irish peatlands. *Ecological Indicators*, 145. <https://doi.org/10.1016/j.ecolind.2022.109731>

- Temmink, R., Lamers, P. M., Angelini, C., & Bouma, T. (2022). Recovering wetland biogeomorphic feedback to restore the world's biotic carbon hotspots. *Science*, 376. <https://doi.org/10.1126/science.abn1479>
- Tian, S., Zhang, X., Tian, J., & Sun, Q. (2016). Random Forest Classification of Wetland Landcovers from Multi-Sensor Data in the Arid Region of Xinjiang, China. *Remote Sensing*, 8(11), Article 11. <https://doi.org/10.3390/rs8110954>
- Tomassen, H. B. M., Smolders, A. J. P., van der Schaaf, S., Lamers, L. P. M., & Roelofs, J. G. M. (2010). Restoration of Raised Bogs: Mechanisms and Case Studies from the Netherlands. In M. Eiselová (Ed.), *Restoration of Lakes, Streams, Floodplains, and Bogs in Europe: Principles and Case Studies* (pp. 285–330). Springer Netherlands. https://doi.org/10.1007/978-90-481-9265-6_15
- Treat, C. C., Kleinen, T., Broothaerts, N., & Dalton, A. S. (2019). Widespread global peatland establishment and persistence over the last 130,000 y. *Proceedings of the National Academy of Sciences*, 116. <https://doi.org/10.1073/pnas.1813305116>
- van Beek, R., Quik, C., & van der Linden, M. (2023). Drowning landscapes revisited. Correlating peatland expansion, human habitation trends and vegetation dynamics in the Northwest European mainland. *Quaternary Science Reviews*, 312. <https://doi.org/10.1016/j.quascirev.2023.108170>
- van Breemen, nico. (1995). How Sphagnum bogs down other plants. *Trends in Ecology & Evolution*, 10. [https://doi.org/10.1016/0169-5347\(95\)90007-1](https://doi.org/10.1016/0169-5347(95)90007-1)
- van Duinen, G. A., Zhuge, Y., Verberk, W. C. E. P., Brock, A. M. T., van Kleef, H. H., Leuven, R. S. E. W., van der Velde, G., & Esselink, H. (2006). Effects of Rewetting Measures in Dutch Raised Bog Remnants on Assemblages of Aquatic Rotifera and Microcrustaceans. *Hydrobiologia*, 565(1), 187–200. <https://doi.org/10.1007/s10750-005-1913-7>

Zou, J., Ziegler, A. D., Chen, D., McNicol, G., Ciais, P., Jiang, X., Zheng, C., Wu, J., Wu, J., Lin, Z., He, X., Brown, L. E., Holden, J., Zhang, Z., Ramchunder, S. J., Chen, A., & Zeng, Z. (2022). Rewetting global wetlands effectively reduces major greenhouse gas emissions. *Nature Geosciences*, *15*. <https://doi.org/10.1038/s41561-022-00989-0>

8. Acknowledgements

I would like to express my upmost gratitude to my supervisor Dr Ralph Temmink for his help, guidance, feedback, patience, and several long drives to collect data and samples.

I would also like to thank Mr. Maarten Zwaarts from the Earths Simulations Lab, Utrecht University, for his help with collecting and processing the drone data and continued help and guidance throughout my analyses.

Also, a big thank you to Mr. Jacob de Bruin and the Team at Natuurmonumenten for providing me with the relevant background information and continuous help throughout the study.

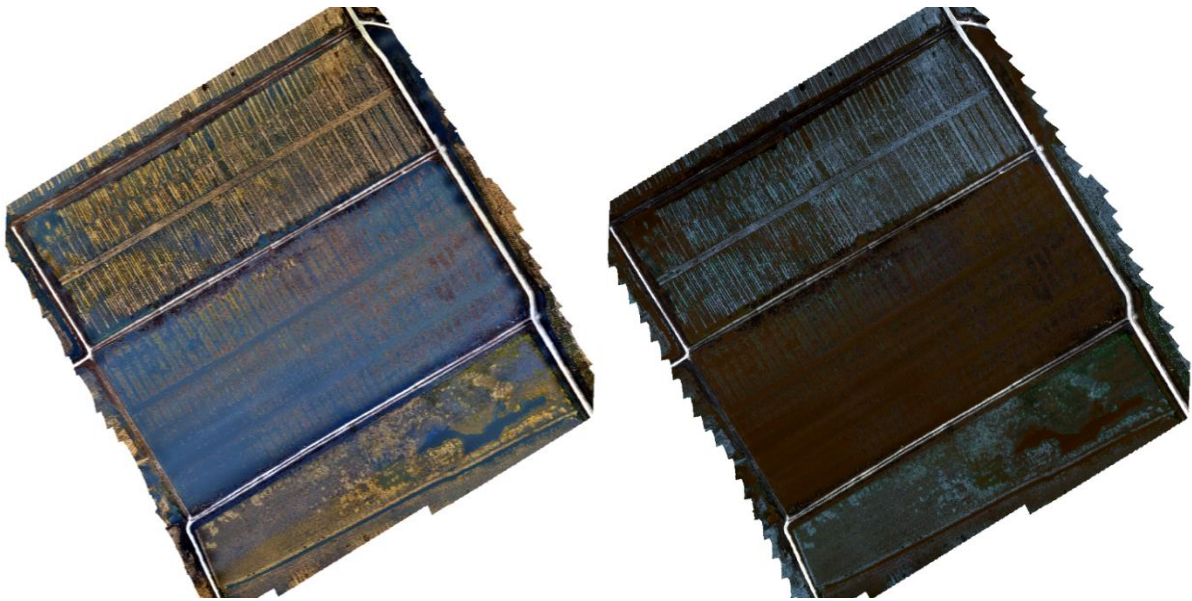
Finally, a big thank you to my friends, family, and girlfriend for all their love and support over the past year.



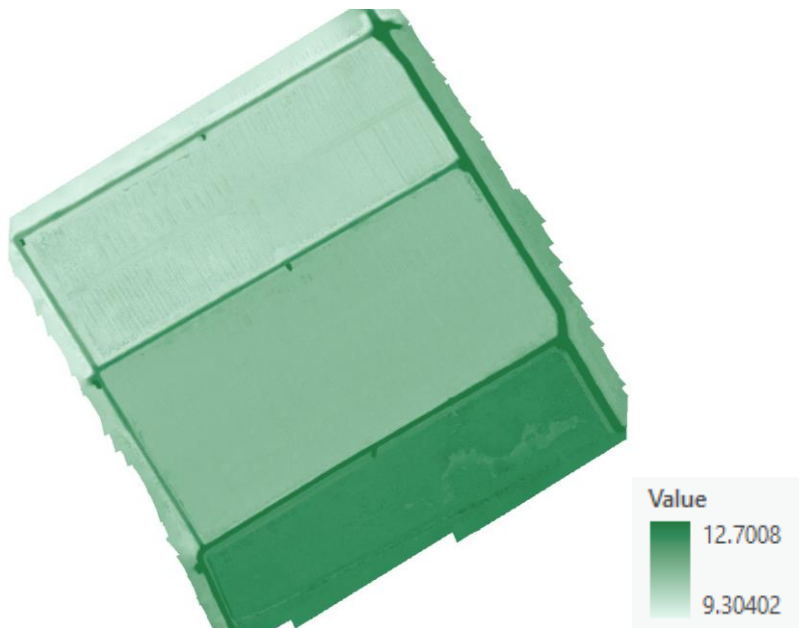
Photo of floating sphagnum patches Temmink, R, 2024.

9. Appendix

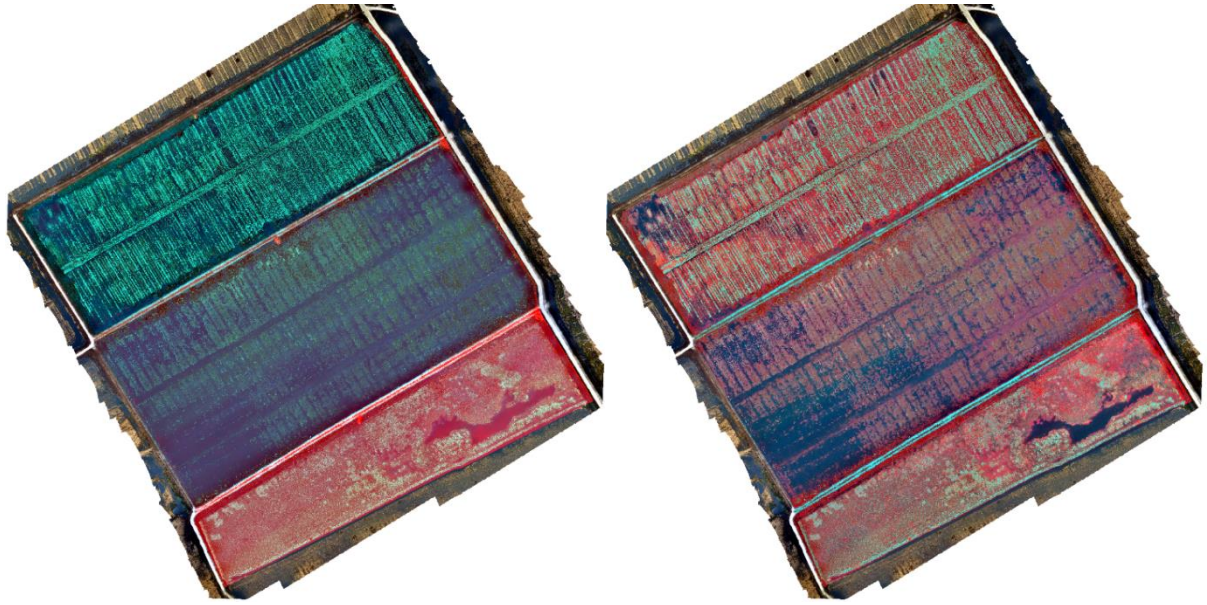
Appendix A- Final Map Rasters



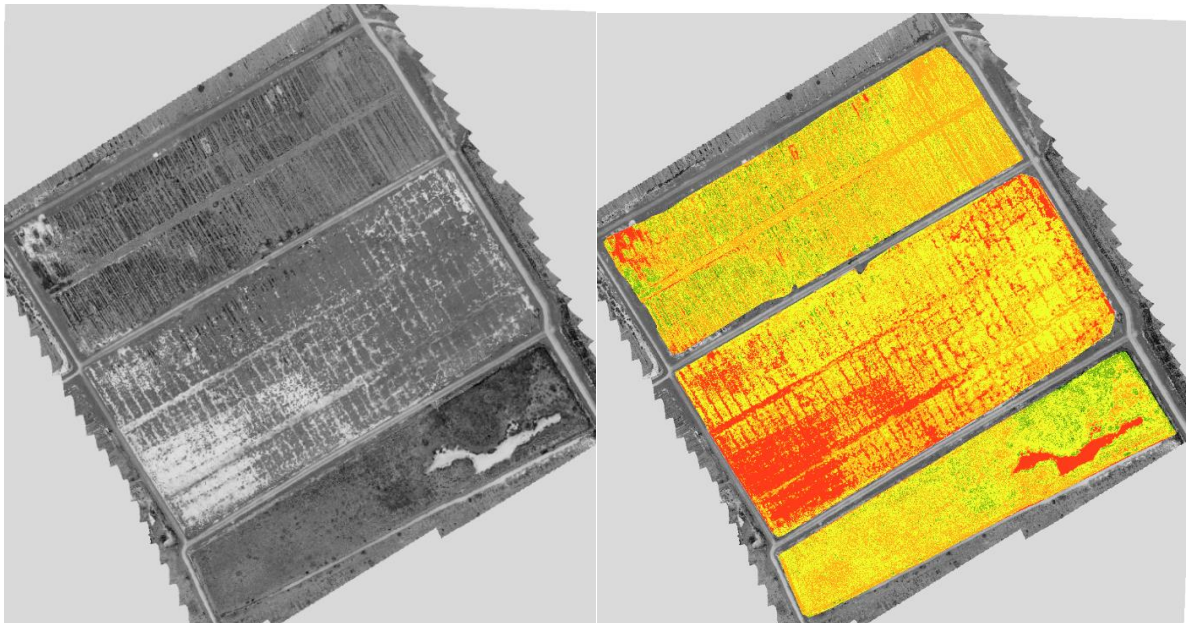
A1. Final RGB Raster Map (left) and Multispectral Raster Map (right)



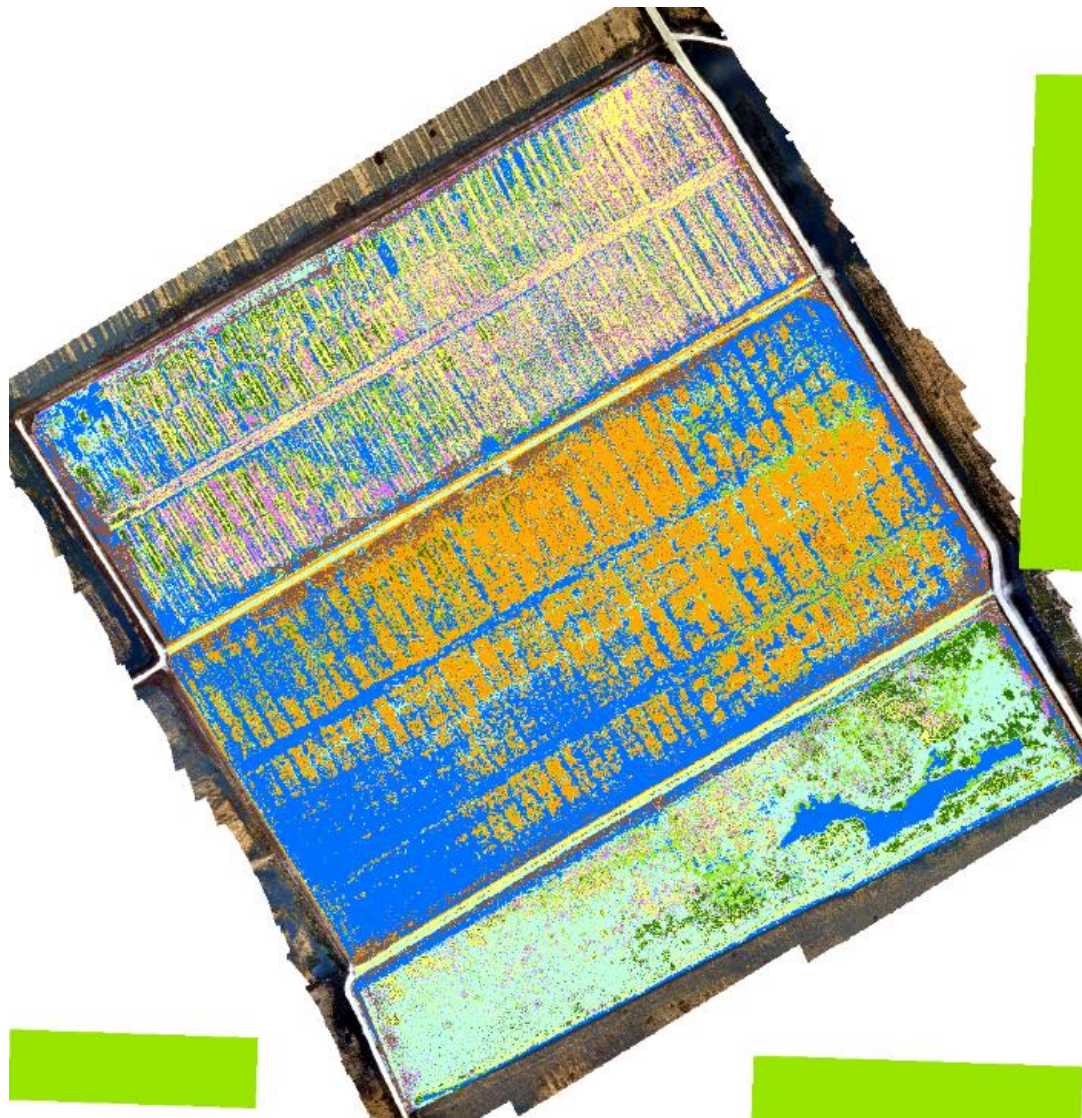
A2. Final DEM Raster Map, Value in meters



A3. Final combination maps, RGB and DEM (left) and RGB, DEM, and NDVI (right)
 RGBDEMNDVI



A4. Final NDVI Maps before reclassification (left) and after (right)



A5. Final classified Map, cause of green bars unknown.

Appendix 2- Precision and Recall for the classification tests

Precision results

Combination tests

<i>RGB</i>	<i>Sphagnum</i>	<i>Molinea</i>	<i>Open water</i>	<i>Bare peat</i>	<i>Cotton Grass</i>	<i>Dead Molinea</i>	<i>Shrubs</i>	<i>Water/Molinea</i>
<i>Test 1</i>	0.52	0.86	0.76	0.90	0.67	0.95	0.71	0.71
<i>Test 2</i>	0.52	0.71	0.86	0.90	0.67	0.86	0.67	0.57
<i>Test 3</i>	0.57	0.81	0.81	0.95	0.71	0.81	0.67	0.43
<i>Test 4</i>	0.48	0.90	0.81	1.00	0.76	0.76	0.81	0.81
<i>Average</i>	0.52	0.82	0.81	0.94	0.70	0.85	0.71	0.63

<i>RGB & DEM</i>	<i>Sphagnum</i>	<i>Molinea</i>	<i>Open water</i>	<i>Bare peat</i>	<i>Cotton Grass</i>	<i>Dead Molinea</i>	<i>Shrubs</i>	<i>Water/Molinea</i>
<i>Test 1</i>	0.62	0.81	0.81	1.00	0.57	0.76	0.71	0.86
<i>Test 2</i>	0.48	0.76	0.71	0.95	0.62	0.90	0.67	0.43
<i>Test 3</i>	0.67	0.71	0.76	1.00	0.57	0.76	0.71	0.62
<i>Test 4</i>	0.71	0.81	0.76	0.95	0.76	0.76	0.86	0.67
<i>Average</i>	0.62	0.77	0.76	0.98	0.63	0.80	0.74	0.64

<i>RGB & NDVI</i>	<i>Sphagnum</i>	<i>Molinea</i>	<i>Open water</i>	<i>Bare peat</i>	<i>Cotton Grass</i>	<i>Dead Molinea</i>	<i>Shrubs</i>	<i>Water/Molinea</i>
<i>Test 1</i>	0.62	0.71	0.71	1.00	0.86	0.76	0.62	0.76
<i>Test 2</i>	0.71	0.86	0.86	0.95	0.76	0.86	0.67	0.71
<i>Test 3</i>	0.76	0.71	0.76	0.95	0.71	0.90	0.81	0.71
<i>Test 4</i>	0.67	0.71	0.81	0.90	0.67	0.86	0.67	0.67
<i>Average</i>	0.69	0.75	0.79	0.95	0.75	0.85	0.69	0.71

<i>RGB, DEM, & NDVI</i>	<i>Sphagnum</i>	<i>Molinea</i>	<i>Open water</i>	<i>Bare peat</i>	<i>Cotton Grass</i>	<i>Dead Molinea</i>	<i>Shrubs</i>	<i>Water/Molinea</i>
<i>Test 1</i>	0.71	0.81	0.90	0.95	0.81	0.81	0.81	0.90
<i>Test 2</i>	0.71	0.81	0.95	0.95	0.90	0.81	0.86	0.90
<i>Test 3</i>	0.76	0.81	0.95	0.90	0.81	0.90	0.90	0.90
<i>Test 4</i>	0.81	0.86	0.95	1.00	0.95	0.86	0.86	0.90
<i>Average</i>	0.75	0.82	0.94	0.95	0.87	0.85	0.86	0.90

Stretch Tests

<i>Sigmoid Level 1</i>	<i>Sphagnum</i>	<i>Molinea</i>	<i>Open water</i>	<i>Bare peat</i>	<i>Cotton Grass</i>	<i>Dead Molinea</i>	<i>Shrubs</i>	<i>Water/Molinea</i>
<i>Test 1</i>	0.62	0.76	1.00	0.95	0.71	0.95	0.90	0.90
<i>Test 2</i>	0.67	0.90	0.90	1.00	0.81	0.95	0.90	0.86
<i>Test 3</i>	0.81	0.95	0.90	0.95	0.71	0.95	1.00	0.90
<i>Test 4</i>	0.67	0.76	0.95	0.95	0.86	0.76	0.81	0.95
<i>Average</i>	0.69	0.85	0.94	0.96	0.77	0.90	0.90	0.90

<i>Sigmoid Level 2</i>	<i>Sphagnum</i>	<i>Molinea</i>	<i>Open water</i>	<i>Bare peat</i>	<i>Cotton Grass</i>	<i>Dead Molinea</i>	<i>Shrubs</i>	<i>Water/Molinea</i>
<i>Test 1</i>	0.71	0.76	0.95	0.90	0.90	0.76	1.00	0.95
<i>Test 2</i>	0.81	0.71	0.90	1.00	0.86	0.81	0.90	0.86
<i>Test 3</i>	0.62	0.81	0.95	0.95	0.86	1.00	0.81	0.95
<i>Test 4</i>	0.67	0.90	1.00	1.00	0.71	0.86	0.90	0.95
<i>Average</i>	0.70	0.80	0.95	0.96	0.83	0.86	0.90	0.93

<i>Min-Max</i>	<i>Sphagnum</i>	<i>Molinea</i>	<i>Open water</i>	<i>Bare peat</i>	<i>Cotton Grass</i>	<i>Dead Molinea</i>	<i>Shrubs</i>	<i>Water/Molinea</i>
<i>Test 1</i>	0.67	0.86	0.95	0.95	0.76	1.00	0.86	0.95
<i>Test 2</i>	0.76	0.81	1.00	0.95	0.95	0.86	0.81	0.86
<i>Test 3</i>	0.81	0.95	0.90	0.95	0.71	0.95	1.00	0.90
<i>Test 4</i>	0.67	0.86	1.00	0.90	0.71	0.90	0.86	0.95
<i>Average</i>	0.73	0.87	0.96	0.94	0.79	0.93	0.88	0.92

Random Forest Depth Tests

<i>Depth 10</i>	<i>Sphagnum</i>	<i>Molinea</i>	<i>Open water</i>	<i>Bare peat</i>	<i>Cotton Grass</i>	<i>Dead Molinea</i>	<i>Shrubs</i>	<i>Water/Molinea</i>
<i>Test 1</i>	0.81	0.86	0.90	0.86	0.71	0.95	0.86	1.00
<i>Test 2</i>	0.81	0.90	0.86	0.90	0.76	0.95	0.81	0.86
<i>Test 3</i>	0.67	0.86	0.81	1.00	0.86	0.76	0.76	0.95
<i>Test 4</i>	0.76	0.81	0.90	0.90	0.57	0.86	0.86	0.90
<i>Average</i>	0.76	0.86	0.87	0.92	0.73	0.88	0.82	0.93

<i>Depth</i> 20	<i>Sphagnum</i>	<i>Molinea</i>	<i>Open water</i>	<i>Bare peat</i>	<i>Cotton Grass</i>	<i>Dead Molinea</i>	<i>Shrubs</i>	<i>Water/Molinea</i>
<i>Test 1</i>	0.71	0.81	0.95	1.00	0.76	0.90	0.86	0.95
<i>Test 2</i>	0.81	0.90	0.95	0.95	0.76	0.76	0.90	0.90
<i>Test 3</i>	0.81	0.90	0.95	0.95	0.76	0.76	0.90	0.90
<i>Test 4</i>	0.76	0.90	1.00	0.95	0.81	0.95	0.81	0.81
<i>Average</i>	0.74	0.88	0.98	0.98	0.79	0.86	0.85	0.88

<i>Depth</i> 30	<i>Sphagnum</i>	<i>Molinea</i>	<i>Open water</i>	<i>Bare peat</i>	<i>Cotton Grass</i>	<i>Dead Molinea</i>	<i>Shrubs</i>	<i>Water/Molinea</i>
<i>Test 1</i>	0.71	0.90	0.95	0.86	0.71	0.76	0.95	0.95
<i>Test 2</i>	0.76	0.86	0.86	1.00	0.90	0.86	0.90	0.81
<i>Test 3</i>	0.76	0.90	1.00	0.86	0.86	0.90	0.90	0.95
<i>Test 4</i>	0.67	0.81	0.90	1.00	0.86	0.95	0.90	0.90
<i>Average</i>	0.73	0.87	0.93	0.93	0.83	0.87	0.92	0.90

<i>Depth</i> 40	<i>Sphagnum</i>	<i>Molinea</i>	<i>Open water</i>	<i>Bare peat</i>	<i>Cotton Grass</i>	<i>Dead Molinea</i>	<i>Shrubs</i>	<i>Water/Molinea</i>
<i>Test 1</i>	0.86	0.86	0.90	0.95	0.71	0.90	0.86	0.86
<i>Test 2</i>	0.62	0.86	0.90	0.86	0.81	0.81	0.90	0.86
<i>Test 3</i>	0.90	0.81	0.90	0.95	0.76	0.81	0.90	0.86
<i>Test 4</i>	0.81	0.86	0.95	0.90	0.86	0.71	0.90	0.90
<i>Average</i>	0.80	0.85	0.92	0.92	0.79	0.81	0.89	0.87

Random Forest Number of trees tests

50 Trees	<i>Sphagnum</i>	<i>Molinea</i>	<i>Open water</i>	<i>Bare peat</i>	<i>Cotton Grass</i>	<i>Dead Molinea</i>	<i>Shrubs</i>	<i>Water/Molinea</i>
<i>Test 1</i>	0.71	0.81	0.90	0.95	0.81	0.81	0.81	0.90
<i>Test 2</i>	0.71	0.81	0.95	0.95	0.90	0.81	0.86	0.90
<i>Test 3</i>	0.76	0.81	0.95	0.90	0.81	0.90	0.90	0.90
<i>Test 4</i>	0.81	0.86	0.95	1.00	0.95	0.86	0.86	0.90
<i>Average</i>	0.75	0.82	0.94	0.95	0.87	0.85	0.86	0.90

100 Trees	<i>Sphagnum</i>	<i>Molinea</i>	<i>Open water</i>	<i>Bare peat</i>	<i>Cotton Grass</i>	<i>Dead Molinea</i>	<i>Shrubs</i>	<i>Water/Molinea</i>
<i>Test 1</i>	0.86	0.90	0.86	0.95	0.67	0.86	0.95	0.90
<i>Test 2</i>	0.71	0.81	0.90	1.00	0.67	0.81	0.95	0.95
<i>Test 3</i>	0.81	0.86	0.86	1.00	0.76	0.76	0.95	0.95
<i>Test 4</i>	0.76	0.90	1.00	1.00	1.00	0.71	0.86	0.76
<i>Average</i>	0.79	0.87	0.90	0.99	0.77	0.79	0.93	0.89

200 Trees	<i>Sphagnum</i>	<i>Molinea</i>	<i>Open water</i>	<i>Bare peat</i>	<i>Cotton Grass</i>	<i>Dead Molinea</i>	<i>Shrubs</i>	<i>Water/Molinea</i>
<i>Test 1</i>	0.76	0.86	0.81	0.90	0.71	0.95	0.86	0.90
<i>Test 2</i>	0.81	0.86	0.95	0.90	0.86	0.81	0.95	1.00
<i>Test 3</i>	0.86	0.86	0.90	1.00	0.76	0.81	0.90	0.95
<i>Test 4</i>	0.67	0.90	0.90	0.86	0.81	0.76	0.90	0.90
<i>Average</i>	0.77	0.87	0.89	0.92	0.79	0.83	0.90	0.94

<i>RGB</i>	<i>Sphagnum</i>	<i>Molinea</i>	<i>Open water</i>	<i>Bare peat</i>	<i>Cotton Grass</i>	<i>Dead Molinea</i>	<i>Shrubs</i>	<i>Water/Molinea</i>
<i>Test 1</i>	0.92	0.82	0.94	0.86	0.70	0.77	0.68	0.56
<i>Test 2</i>	0.85	0.71	0.95	0.86	0.52	0.82	0.70	0.50
<i>Test 3</i>	0.80	0.77	0.85	0.83	0.60	0.85	0.54	0.56
<i>Test 4</i>	0.83	0.83	0.85	0.91	0.70	0.89	0.65	0.74
<i>Average</i>	0.85	0.78	0.90	0.87	0.63	0.83	0.64	0.59
<i>300 Trees</i>	<i>Sphagnum</i>	<i>Molinea</i>	<i>Open water</i>	<i>Bare peat</i>	<i>Cotton Grass</i>	<i>Dead Molinea</i>	<i>Shrubs</i>	<i>Water/Molinea</i>
<i>Test 1</i>	0.67	0.86	1.00	0.95	0.67	0.86	0.86	0.86
<i>Test 2</i>	0.81	0.90	1.00	0.90	0.76	0.90	0.86	0.86
<i>Test 3</i>	0.71	0.95	0.90	0.95	0.81	0.86	0.95	0.90
<i>Test 4</i>	0.76	0.86	0.95	1.00	0.86	0.86	0.81	0.95
<i>Average</i>	0.74	0.89	0.96	0.95	0.77	0.87	0.87	0.89
<i>400 Trees</i>	<i>Sphagnum</i>	<i>Molinea</i>	<i>Open water</i>	<i>Bare peat</i>	<i>Cotton Grass</i>	<i>Dead Molinea</i>	<i>Shrubs</i>	<i>Water/Molinea</i>
<i>Test 1</i>	0.76	0.86	0.95	0.95	0.81	0.86	0.86	0.90
<i>Test 2</i>	0.86	0.86	0.90	0.95	0.86	0.86	0.95	0.95
<i>Test 3</i>	0.76	0.86	0.95	0.95	0.90	0.81	0.81	0.86
<i>Test 4</i>	0.76	0.86	0.95	1.00	0.86	0.86	0.81	0.95
<i>Average</i>	0.79	0.86	0.94	0.96	0.86	0.85	0.86	0.92

Recall results

Combination tests

<i>RGB & DEM</i>	<i>Sphagnum</i>	<i>Molinea</i>	<i>Open water</i>	<i>Bare peat</i>	<i>Cotton Grass</i>	<i>Dead Molinea</i>	<i>Shrubs</i>	<i>Water/Molinea</i>
<i>Test 1</i>	0.68	0.77	0.89	0.91	0.67	0.89	0.68	0.67
<i>Test 2</i>	0.91	0.76	0.71	1.00	0.59	0.86	0.58	0.33
<i>Test 3</i>	0.78	0.75	0.80	0.95	0.57	0.89	0.63	0.52
<i>Test 4</i>	0.79	0.77	0.89	0.91	0.76	0.76	0.82	0.61
<i>Average</i>	0.79	0.76	0.82	0.94	0.65	0.85	0.68	0.53

<i>RGB & NDVI</i>	<i>Sphagnum</i>	<i>Molinea</i>	<i>Open water</i>	<i>Bare peat</i>	<i>Cotton Grass</i>	<i>Dead Molinea</i>	<i>Shrubs</i>	<i>Water/Molinea</i>
<i>Test 1</i>	0.72	0.71	0.88	0.95	0.82	0.73	0.65	0.62
<i>Test 2</i>	0.83	0.78	0.95	1.00	0.94	0.75	0.70	0.56
<i>Test 3</i>	0.84	0.74	1.00	1.00	0.85	0.83	0.86	0.86
<i>Test 4</i>	0.85	0.90	1.00	0.88	0.95	0.86	0.86	0.90
<i>Average</i>	0.82	0.83	0.98	0.90	0.85	0.82	0.90	0.86

<i>RGB, DEM, & NDVI</i>	<i>Sphagnum</i>	<i>Molinea</i>	<i>Open water</i>	<i>Bare peat</i>	<i>Cotton Grass</i>	<i>Dead Molinea</i>	<i>Shrubs</i>	<i>Water/Molinea</i>
<i>Test 1</i>	0.71	0.85	0.95	0.87	0.85	0.81	0.94	0.76
<i>Test 2</i>	0.88	0.85	0.95	0.87	0.76	0.77	0.95	0.90
<i>Test 3</i>	0.84	0.74	1.00	1.00	0.85	0.83	0.86	0.86
<i>Test 4</i>	0.85	0.90	1.00	0.88	0.95	0.86	0.86	0.90
<i>Average</i>	0.82	0.83	0.98	0.90	0.85	0.82	0.90	0.86

Stretch Tests

<i>Sigmoid Level 1</i>	<i>Sphagnum</i>	<i>Molinea</i>	<i>Open water</i>	<i>Bare peat</i>	<i>Cotton Grass</i>	<i>Dead Molinea</i>	<i>Shrubs</i>	<i>Water/Molinea</i>
<i>Test 1</i>	0.76	0.94	0.95	0.91	0.83	0.80	0.95	0.70
<i>Test 2</i>	0.88	0.76	0.86	0.91	1.00	0.87	1.00	0.78
<i>Test 3</i>	0.81	0.95	0.90	0.95	0.94	0.91	0.91	0.83
<i>Test 4</i>	0.70	0.94	0.87	0.91	0.78	0.84	0.94	0.77
<i>Average</i>	0.79	0.90	0.90	0.92	0.89	0.86	0.95	0.77

<i>Sigmoid Level 2</i>	<i>Sphagnum</i>	<i>Molinea</i>	<i>Open water</i>	<i>Bare peat</i>	<i>Cotton Grass</i>	<i>Dead Molinea</i>	<i>Shrubs</i>	<i>Water/Molinea</i>
<i>Test 1</i>	0.83	0.89	0.87	0.95	0.83	0.89	0.95	0.77
<i>Test 2</i>	0.85	0.83	0.95	0.88	0.86	0.89	0.90	0.72
<i>Test 3</i>	1.00	0.77	0.91	0.87	0.82	0.84	0.89	0.91
<i>Test 4</i>	0.82	0.83	0.91	0.91	0.83	0.90	0.90	0.87
<i>Average</i>	0.88	0.83	0.91	0.90	0.83	0.88	0.91	0.82

<i>Min-Max</i>	<i>Sphagnum</i>	<i>Molinea</i>	<i>Open water</i>	<i>Bare peat</i>	<i>Cotton Grass</i>	<i>Dead Molinea</i>	<i>Shrubs</i>	<i>Water/Molinea</i>
<i>Test 1</i>	0.93	1.00	0.95	0.87	0.89	0.75	0.95	0.77
<i>Test 2</i>	0.89	0.85	1.00	0.91	0.80	0.78	0.94	0.86
<i>Test 3</i>	0.81	0.95	0.90	0.95	0.94	0.91	0.91	0.83
<i>Test 4</i>	0.93	0.86	0.95	0.79	0.83	0.83	0.86	0.83
<i>Average</i>	0.89	0.91	0.95	0.88	0.86	0.82	0.92	0.82

Random Forest Depth Tests

<i>Depth 10</i>	<i>Sphagnum</i>	<i>Molinea</i>	<i>Open water</i>	<i>Bare peat</i>	<i>Cotton Grass</i>	<i>Dead Molinea</i>	<i>Shrubs</i>	<i>Water/Molinea</i>
<i>Test 1</i>	0.81	0.95	0.90	0.90	0.94	0.91	0.86	0.75
<i>Test 2</i>	0.85	0.86	1.00	0.86	0.94	0.83	0.81	0.75
<i>Test 3</i>	0.74	0.95	0.94	0.81	0.86	0.76	0.89	0.77
<i>Test 4</i>	0.76	0.85	0.95	0.79	0.86	0.78	0.82	0.79
<i>Average</i>	0.79	0.90	0.95	0.84	0.90	0.82	0.84	0.77

<i>Depth 20</i>	<i>Sphagnum</i>	<i>Molinea</i>	<i>Open water</i>	<i>Bare peat</i>	<i>Cotton Grass</i>	<i>Dead Molinea</i>	<i>Shrubs</i>	<i>Water/Molinea</i>
<i>Test 1</i>	0.75	0.94	0.95	0.88	0.89	0.83	0.95	0.80
<i>Test 2</i>	0.77	0.86	1.00	0.91	0.84	0.80	0.90	0.86
<i>Test 3</i>	0.78	0.90	0.88	0.91	0.77	0.74	1.00	0.90
<i>Test 4</i>	0.89	0.83	0.95	0.87	0.85	0.83	0.94	0.85
<i>Average</i>	0.80	0.88	0.95	0.89	0.84	0.80	0.95	0.85

<i>Depth 30</i>	<i>Sphagnum</i>	<i>Molinea</i>	<i>Open water</i>	<i>Bare peat</i>	<i>Cotton Grass</i>	<i>Dead Molinea</i>	<i>Shrubs</i>	<i>Water/Molinea</i>
<i>Test 1</i>	0.83	0.86	0.91	0.82	0.88	0.84	0.83	0.83
<i>Test 2</i>	0.89	0.82	1.00	0.95	0.83	0.78	0.95	0.77
<i>Test 3</i>	0.89	0.95	0.91	0.90	0.90	0.90	0.86	0.83
<i>Test 4</i>	0.93	0.89	0.90	0.88	0.86	0.77	0.95	0.86
<i>Average</i>	0.89	0.88	0.93	0.89	0.87	0.82	0.90	0.83

<i>Depth</i> 40	<i>Sphagnum</i>	<i>Molinea</i>	<i>Open</i> <i>water</i>	<i>Bare</i> <i>peat</i>	<i>Cotton</i> <i>Grass</i>	<i>Dead</i> <i>Molinea</i>	<i>Shrubs</i>	<i>Water/Molinea</i>
<i>Test 1</i>	0,82	0,82	1,00	0,91	0,68	0,90	0,95	0,86
<i>Test 2</i>	0,81	0,82	0,90	0,95	0,77	0,71	0,90	0,78
<i>Test 3</i>	0,83	0,89	1,00	0,91	0,73	0,89	0,90	0,78
<i>Test 4</i>	0,81	0,82	0,95	0,86	0,86	0,83	0,90	0,86
<i>Average</i>	0,82	0,84	0,96	0,91	0,76	0,84	0,92	0,82

Random Forest Number of trees tests

50 <i>Trees</i>	<i>Sphagnum</i>	<i>Molinea</i>	<i>Open</i> <i>water</i>	<i>Bare</i> <i>peat</i>	<i>Cotton</i> <i>Grass</i>	<i>Dead</i> <i>Molinea</i>	<i>Shrubs</i>	<i>Water/Molinea</i>
<i>Test 1</i>	0,71	0,85	0,95	0,87	0,85	0,81	0,94	0,76
<i>Test 2</i>	0,88	0,85	0,95	0,87	0,76	0,77	0,95	0,90
<i>Test 3</i>	0,84	0,74	1,00	1,00	0,85	0,83	0,86	0,86
<i>Test 4</i>	0,85	0,90	1,00	0,88	0,95	0,86	0,86	0,90
<i>Average</i>	0,82	0,83	0,98	0,90	0,85	0,82	0,90	0,86

100 <i>Trees</i>	<i>Sphagnum</i>	<i>Molinea</i>	<i>Open</i> <i>water</i>	<i>Bare</i> <i>peat</i>	<i>Cotton</i> <i>Grass</i>	<i>Dead</i> <i>Molinea</i>	<i>Shrubs</i>	<i>Water/Molinea</i>
<i>Test 1</i>	0,86	0,86	0,86	0,87	0,88	0,86	0,87	0,90
<i>Test 2</i>	0,88	0,77	1,00	0,91	0,74	0,74	0,95	0,83
<i>Test 3</i>	0,81	0,90	0,95	0,88	0,84	0,80	0,95	0,83
<i>Test 4</i>	0,76	0,95	0,91	0,95	0,81	0,79	0,95	0,89
<i>Average</i>	0,83	0,87	0,93	0,90	0,82	0,80	0,93	0,87

200 <i>Trees</i>	<i>Sphagnum</i>	<i>Molinea</i>	<i>Open</i> <i>water</i>	<i>Bare</i> <i>peat</i>	<i>Cotton</i> <i>Grass</i>	<i>Dead</i> <i>Molinea</i>	<i>Shrubs</i>	<i>Water/Molinea</i>
<i>Test 1</i>	0,81	0,89	0,91	0,79	0,84	0,78	0,85	0,80
<i>Test 2</i>	0,79	0,86	0,95	0,95	0,83	0,87	0,86	0,84
<i>Test 3</i>	0,81	0,86	0,88	0,83	0,80	0,79	0,94	0,90
<i>Test 4</i>	0,88	0,78	0,95	0,91	0,88	0,77	0,95	0,76
<i>Average</i>	0,82	0,85	0,92	0,87	0,84	0,80	0,90	0,83

300 <i>Trees</i>	<i>Sphagnum</i>	<i>Molinea</i>	<i>Open</i> <i>water</i>	<i>Bare</i> <i>peat</i>	<i>Cotton</i> <i>Grass</i>	<i>Dead</i> <i>Molinea</i>	<i>Shrubs</i>	<i>Water/Molinea</i>
<i>Test 1</i>	0,84	0,75	0,94	0,90	0,94	0,83	0,90	0,73
<i>Test 2</i>	0,85	0,86	0,95	0,95	0,95	0,94	0,91	0,78
<i>Test 3</i>	0,90	0,86	1,00	0,91	0,76	0,81	0,95	0,87
<i>Test 4</i>	0,70	0,95	0,95	0,90	0,77	0,76	0,86	0,83
<i>Average</i>	0,82	0,85	0,96	0,92	0,85	0,84	0,91	0,80

400 <i>Trees</i>	<i>Sphagnum</i>	<i>Molinea</i>	<i>Open</i> <i>water</i>	<i>Bare</i> <i>peat</i>	<i>Cotton</i> <i>Grass</i>	<i>Dead</i> <i>Molinea</i>	<i>Shrubs</i>	<i>Water/Molinea</i>
<i>Test 1</i>	0,78	0,78	0,95	0,87	0,74	0,86	0,90	0,82
<i>Test 2</i>	0,89	0,86	0,91	0,90	0,94	0,86	0,90	0,75
<i>Test 3</i>	0,79	0,95	1,00	0,87	0,94	0,86	0,87	0,79
<i>Test 4</i>	0,84	0,86	0,95	0,88	0,78	0,90	1,00	0,87
<i>Average</i>	0,83	0,86	0,95	0,88	0,85	0,87	0,92	0,81

